

# USING THE HVSR, MASW, AND SEISMIC REFRACTION ANALYSIS METHODS TO ESTIMATE THE SUBSURFACE SEISMIC STRUCTURES OF TWO EARTH EMBANKMENT DAMS

Steven J. Maniscalco



A thesis

submitted to the Faculty of

the department of Earth and Environmental Sciences

in partial fulfillment

of the requirements for the Bachelor of Science degree of

Environmental Geoscience

Boston College  
Morrissey College of Arts and Sciences  
Undergraduate Programs

April, 2023

# **USING THE HVSR, MASW, AND SEISMIC REFRACTION ANALYSIS METHODS TO ESTIMATE THE SUBSURFACE SEISMIC STRUCTURES OF TWO EARTH EMBANKMENT DAMS**

Steven J. Maniscalco

Advisor: Prof. John E. Ebel, Ph.D.

## **ABSTRACT**

Degradation within an earth embankment structure is often unobservable from the surface. In order to evaluate the structural integrity of earth embankment dams and levees and identify subsurface zones of weakness that may result in future failures, various geophysical methods have been proposed as effective subsurface imaging tools. This study presents the results of using the horizontal-to-vertical spectral ratio (HVSr), seismic refraction analysis, and multi-channel analysis of surface waves (MASW) methods to estimate subsurface seismic structures for two earth embankment dams located in Chestnut Hill, MA, and Franklin Falls, NH. The estimated seismic velocity structures from the seismic refraction analysis and MASW performed in this study confirm the HVSr method is able to effectively estimate depth to bedrock at sites atop earth embankments using estimated fundamental frequencies. The MASW was found to resolve a low-velocity zone in the subsurface at the Chestnut Hill Reservoir embankment that the seismic refraction method was unable to image, and this low-velocity zone is required to best fit a theoretical HVSr to an observed spectrum. Furthermore, the variation and uncertainty in fundamental frequency estimation were investigated by making repeated HVSr measurements at the Chestnut Hill embankment.

## **Acknowledgements**

First and foremost, I would like to extend my sincere gratitude to my advisor Professor John E. Ebel. Since my freshman year when I was first his student, Professor Ebel has challenged me to do my best work and has always encouraged me to strive for improvement. I have learned a lot from him about what it means to be a good scientist, and from his mentorship I have grown immensely as an academic and individual. I will forever be grateful to Professor Ebel for taking me under his wing and guiding me through my undergraduate studies.

I would like to thank Marshall Pontrelli, Yueqian Wang, William Doll, and Janet Simms for their vital collaboration and contributions to this research. It has been a pleasure getting to know all of them, and I am thankful for the knowledge, advice, and kindness they have shared with me. I would like to thank the U.S. Army Corps of Engineers Engineer Research and Development Center for funding the research I have been so lucky to be a part of. I would also like to express my gratitude to the department of Earth and Environmental Sciences at Boston College for fostering an atmosphere of inclusiveness, learning, and enthusiasm in and outside the classroom.

Finally, I cannot thank my family and friends enough for their endless support and encouragement in pursuing my passions. I can always count on those around me to hold me up in times of need and bring a smile to my face. I would like to thank my mom, dad, and brother for shaping me into the person I am today and making it possible for me to succeed. I am forever grateful to you all.

## Introduction

Earth embankment levees and dams are vital infrastructure used to protect life and property from extreme flood events. When these structures fail, disaster can ensue with high death tolls and costly damages. It is therefore a priority to develop methods to evaluate the structural integrity of such earth embankment structures, which degrade due to natural processes over time. Because much of this degradation within earth embankment structures is not observable from the surface, geophysical methods have been proposed as effective options to evaluate subsurface degradation. Through geophysical methods, seismic properties like seismic-wave velocities, densities, and thicknesses of subsurface layers can be estimated. Geophysical measurements allow for spatial or temporal changes in these subsurface properties to be estimated, which could indicate subsurface degradation within an earth embankment structure from processes like erosion or infiltration. Exploring geophysical methods to identify areas of weakness within earth embankment structures is desirable because many such methods are inexpensive, noninvasive, and fast to implement. Using the geophysical methods of HVSR, seismic refraction analysis, and MASW as well as by modeling subsurface seismic structure, we aim to estimate the values and uncertainties of P-wave velocities, S-wave velocities, densities, and thicknesses of subsurface layers that lie above bedrock below the earth embankment structures at the Chestnut Hill Reservoir in Massachusetts and Franklin Falls Dam in New Hampshire. We also aim to investigate how these subsurface seismic properties might vary with time and reservoir water level at the Chestnut Hill Reservoir.

The geophysical methods of HVSR, seismic refraction analysis, and MASW have been widely applied to image subsurface seismic structures. Seismic refraction analysis and MASW (multi-channel analysis of surface waves) have been used to characterize shallow subsurface

seismic structures. Both methods are typically employed to determine seismic properties of layers at depths down to 30 m. Refraction analysis is commonly employed at sites where the geology is not complex because the method cannot detect low-velocity zones nor lateral changes in seismic velocities. Low-velocity zones cannot be detected by refraction because rays entering a lower-velocity layer from an overlying higher-velocity layer are never critically (horizontally) refracted through the lower velocity layer, and thus no head waves are generated at that layer boundary (Dobrin, 1976). This results in overestimation of the thickness of the higher-velocity layer above the low-velocity layer as well as the depths of layers under the lower-velocity layer. Due to this limitation of refraction analysis, MASW is generally favored for mapping layer thicknesses, S-wave velocities, and densities (Kesarwani et al., 2012).

Nakamura (1989) originally proposed the HVSR (horizontal-to-vertical spectral ratio) method as a means to estimate the amplification of seismic waves due to a site's surficial soil layers. In addition to ground-shaking amplification research, applications of the method have broadened since its introduction to site classification, mineral exploration, and estimation of subsurface S-wave velocity structure (Xu & Wang, 2021). Studies such as those carried out by Bignardi (2017) and Moon et al. (2019) have found the HVSR method to be successful in estimating depth to bedrock below a surface assuming a single soft sedimentary layer overlying a faster bedrock layer. However, less is known about the resolution at which seismic properties of individual layers within this single assumed soft sedimentary layer can be characterized when using HVSRs. Furthermore, there is limited documentation of repeated HVSR measurements at a single site over time, so little is known about variation within a set of repeated HVSRs at a site. This study aims to address these uncertainties.

## Measurement Sites

### Chestnut Hill Reservoir

Most of the data included in this study were collected from the Chestnut Hill, Massachusetts Reservoir embankment. The geographic location and a picture of the embankment are shown in Figure 1. The Chestnut Hill Reservoir was constructed in 1866-1870 and was historically used as a public water supply to the City of Boston (Boston Landmarks Commission, 1989, p. 5). Today, the reservoir is owned by the Massachusetts Water Resources Authority (MWRA) and managed by the Department of Conservation and Recreation (DCR). The reservoir no longer serves as an active water supply, although it remains as a backup option (Massachusetts Department of Conservation and Recreation, 2006, p. ix). The reservoir site was originally a natural basin with marsh and meadow lands (Massachusetts DCR, 2006, p. 5). The underlying bedrock geology of the reservoir area is known as the Roxbury Conglomerate or Roxbury Puddingstone (Massachusetts DCR, 2006, p. 2), and outcrops of this bedrock are visible in the northeast section of the reservoir area. The manmade earth embankment on which measurements were conducted is located on the east side of the reservoir, reaching a maximum height of approximately 6-7 m or roughly 20 ft at its northern end and gradually decreasing to ground level at its southern end (Figure 2). According to the 1989 *Chestnut Hill Reservoir and Pump Stations* report, the inner slope (reservoir side) of the embankment is “capped with granite blocks about 3 feet below the top of the embankment” (Boston Landmarks Commission, 1989, p. 6). These granite blocks (pictured in Figure 3) can be seen at the site sitting just below the top of the embankment and extending inward from its inner-slope side. The extent to which these blocks extend into the embankment can only be speculated, but it is also possible that additional blocks or a compact layer of rock fill line the crest of the embankment below the gravel path, a

common practice for reinforcing earth embankment structures (U.S. Army Corps of Engineers, 2004). The embankment runs adjacent to high-traffic Beacon Street. A gravel path lines the top of the embankment and is approximately 3 m (~10 ft) wide in all places. Recreational walkers and runners frequent the path throughout the year.

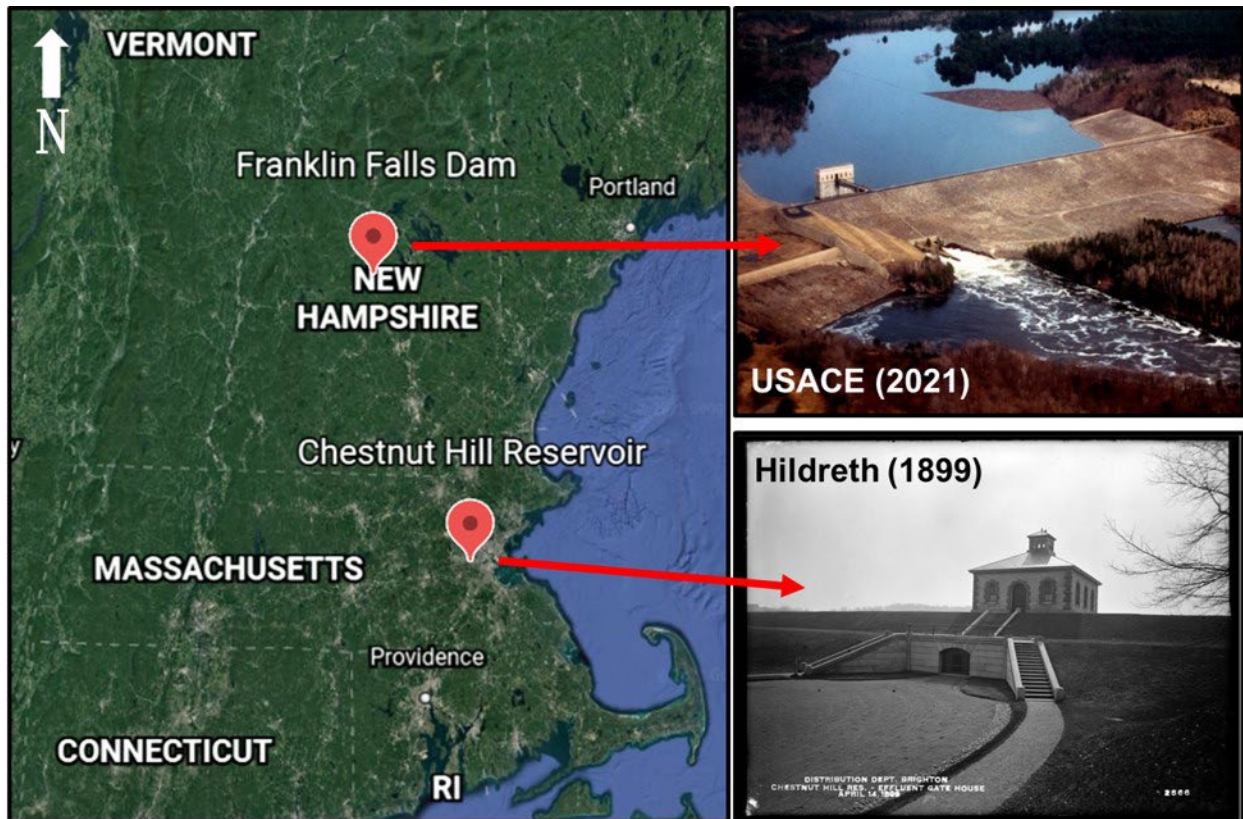


**Figure 1.** (left) Geographic locations of the Chestnut Hill Reservoir (Chestnut Hill, Massachusetts) and Franklin Falls Dam (Franklin, New Hampshire) measurement sites in the northeast United States. (right) Pictures of the Franklin Falls Dam (top) and Chestnut Hill Reservoir embankment (bottom). The thickest part of the Chestnut Hill Reservoir embankment is pictured.

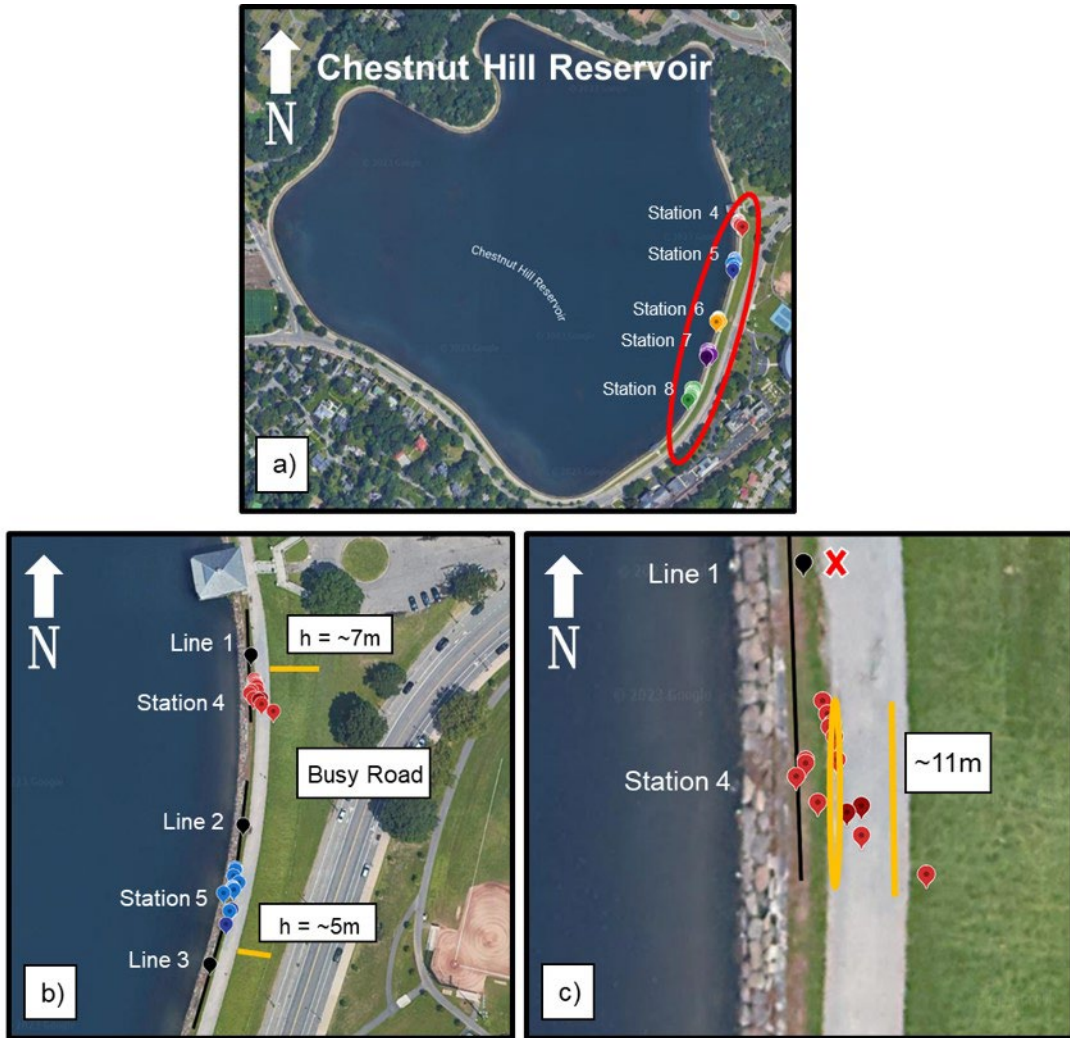


**Figure 2.** **a)** Repeated ambient seismic noise measurements were made along the manmade embankment on the east side of the reservoir (circled in red) at Stations 4-8. All measurements at these stations are pinned, color coded, and labeled. Embankment thickness gradually decreases to about ground level at the southern end of the red circle. **b)** The embankment is thickest near Station 4 at a height of about 7 m above ground level and gradually decreases in thickness in the southern direction. Seismic refraction/MASW Lines 1-3, are shown in black and labeled at their midpoints. Beacon street is pictured to the right of the embankment and is highly trafficked. **c)** Station 4 measurement locations as recorded by GPS. The measurements were made at the edge of the gravel path on the inner-slope side of the embankment (circled in yellow). The measurements for Station 4 were all made within 11 m of each other. The red “X” represents a Station 4 measurement that was excluded from the analysis because it is more than 20 m from any measurement of the same station.

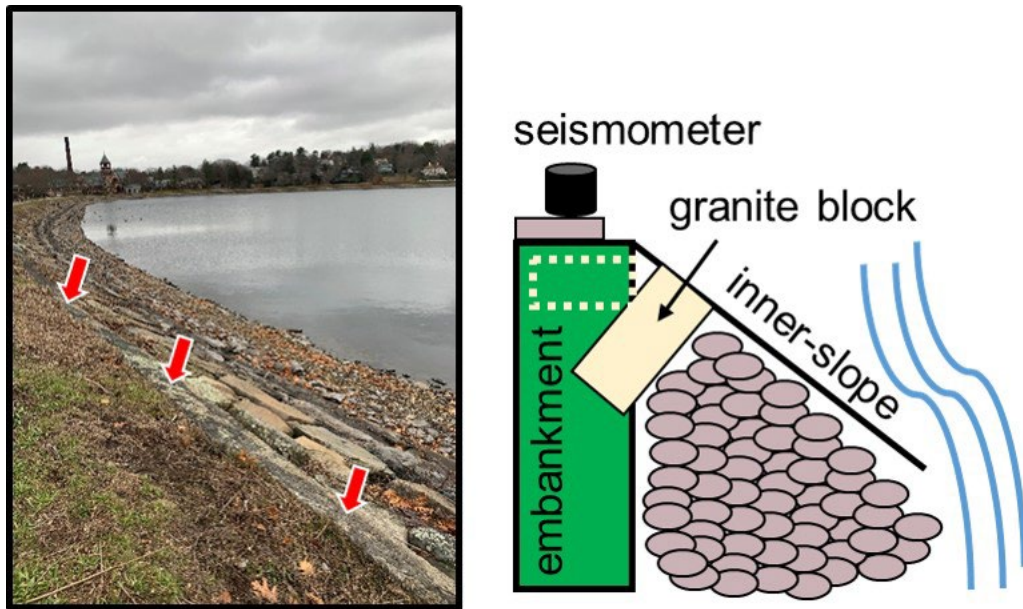


**Figure 3. (left)** The inner-slope of the Chestnut Hill Reservoir embankment is capped with granite blocks (indicated with red arrows) that extend into the embankment. **(right)** A cross-sectional diagram of the embankment and placement of the seismometer during ambient seismic noise data collection is shown. The hidden dimensions of the granite blocks can only be speculated on, and the dotted box indicates a possible location of a block or rockfill layer that could have been used to reinforce the embankment.

### Franklin Falls Dam

The Franklin Falls Dam is located on the Pemigewasset River in Franklin, New Hampshire (geographic location and picture shown in Figure 1). The dam is an earth embankment that stands approximately 43 m (140 ft) tall and is about 6.7 m (22 ft) wide at its top (Figure 4). The earthfill dam features stone slope protection and a concrete weir chute spillway founded on rock (United States Army Corps of Engineers, 2021). The dam was constructed by USACE from 1939-1943 as part of a flood risk management plan for the Merrimack River Basin. As of 2011, USACE (2021) estimates that the project has prevented \$178.3 million in flood damages since its construction, showcasing the vital role earth embankments serve and the importance of monitoring the structural integrity of such infrastructure.

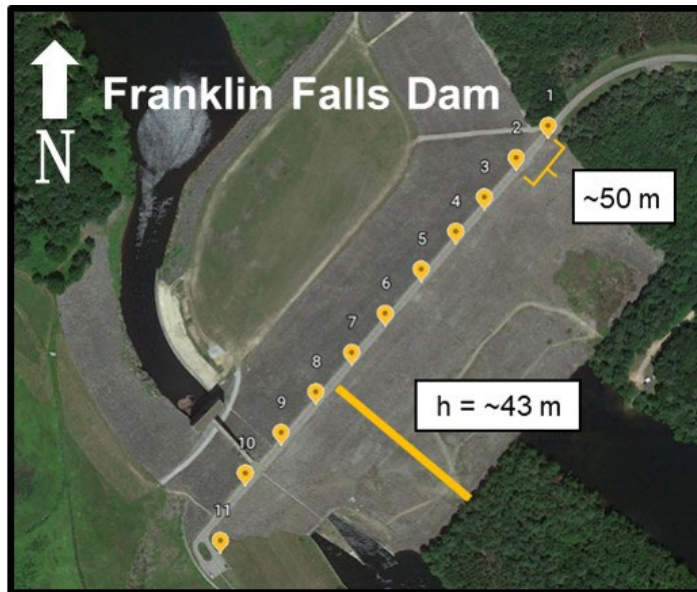


**Figure 4.** A single set of ambient seismic noise collections was made at the Franklin Falls Dam. The locations of these noise collections (with approximately 50 m spacing) were recorded via GPS and are indicated by yellow markers. The height of the dam is fairly constant and is about 43 m above the water surface of the Pemigewasset River.

## Methods

### HVSR

The horizontal-to-vertical spectral ratio seismological method, commonly referred to as the H/V spectral ratio or HVSR, was proposed by Nakamura (1989) to estimate the potential of a site to amplify earthquake ground motions due to resonances in the near-surface soil layers. HVSRs can be calculated from ambient seismic noise recordings with time lengths on the order of tens of minutes. Using two horizontal components and the vertical components from observed seismic noise waveforms, a fundamental frequency can be determined for an observation site and depth to bedrock can be estimated, even in the presence of limited artificial tremors such as footsteps (Nakamura, 1989). A site's fundamental frequency has several applications, one of which is to estimate depth to bedrock. The depth from the surface to bedrock can be determined by the following equation (adapted from Lane et al., 2008):

$$h_{min} = \frac{V_{surface}}{4 \cdot f_0} \quad \text{Eq. (1)}$$

where  $h_{min}$  is the thickness of the layer over the bedrock,  $V_{surface}$  is the average shear-wave velocity of the sediment layer above bedrock, and  $f_0$  is the fundamental frequency determined from a site's HVSR. This equation assumes a 2-layer model consisting of one slower  $V_s$  layer of sediment above a faster  $V_s$  bedrock layer (Lane et al., 2008, 2).

Ambient seismic noise was recorded along the top of the manmade earth embankment on the east side of the Chestnut Hill Reservoir in order to provide data to help evaluate how well the HVSR method could be used to estimate depth to bedrock. The seismometer was placed on the inner-slope side of the gravel path (circled in Figure 2) that runs along the top of the reservoir embankment, and each data recording was about 20 minutes long. Repeated measurements were made at Stations 4-8 (shown in Figure 2) on the embankment to investigate the natural variations of site fundamental frequencies along the thicker section of the dam. The stations span the majority of the manmade embankment and are located at thicknesses ranging from approximately 7 m to 3 m. When they were reoccupied, the positions of the five stations were estimated by pacing out distances between stations and keeping track of each recording location's GPS coordinates. Ideally, visual markers (such as flags) would have been used to precisely mark the positions of the stations for reoccupation, but it was not possible to place markers on this public path. The approximate method of reoccupying station locations using pacing from a known location resulted in the stations being at somewhat different locations from one reoccupation to the next. For example, site position varied by about 7 m for Station 6 but varied by nearly 20 m for Stations 5 and 8. Site position variation at each station is thus a source of variation in the fundamental frequency values from one measurement to the next.

In total, seventeen sets of repeated ambient noise recordings were made at the five stations on different days from July 2021 to December 2022. Most of the recordings were made during July and August of 2021, with a few recordings also being made in September 2021 and March 2022. The average water level was about 131.6 ft during these measurements and varied by less than 1.0 ft between measurements. The data contains two sets of recordings when the average reservoir water level was about 125.5 ft (~6 ft lower than that of the other measurements) in December 2021 and December 2022 due to planned water level drawdowns by the MWRA. The average water levels for the Chestnut Hill Reservoir were derived from daily water level data, measured in elevation above sea level, provided by the MWRA. The non-December measurements will hereby be referred to as normal water level measurements and the December measurements as low water level measurements. It should be noted that data from every station were not always recovered during each set of recordings, as data were occasionally lost to equipment malfunctions or discarded if the measurement was made more than 20 m from other measurement locations for the same station. An example of a condition for which a measurement was discarded is shown in Figure 2. Because of this, some stations have more data than others, but each station has at least ten repeated recordings made within 20 m or less of each other included in this analysis.

A single set of ambient seismic noise recordings was also made at eleven stations along the Franklin Falls Dam on August 20, 2021. The stations spanned the length of the dam and are shown in Figure 4. HVSRs were calculated for each station on the Franklin Falls Dam, which is much taller than the Chestnut Hill Reservoir embankment, to see if accurate depth to bedrock estimates could be made at the dam from the HVSR method.

The ambient seismic noise recordings, which each lasted 20 minutes, sampled the North-South, East-West, and Vertical components of waves at a sample rate of 100 Hz. The data were then processed to produce HVSR curves using a MATLAB script written by Pontrelli (2020). Figure 5 provides a flowchart of the data processing and computations. Raw noise data are filtered using a fourth-order bandpass Butterworth filter (Butterworth, 1930) with a low corner of 0.1 Hz and high corner of 49 Hz. The data are broken up into 27 windows with 40 second lengths, each with a spacing of 1 second between windows. However, the first window of each measurement is removed to reduce manmade noise caused by initially handling the seismometer. The Fourier spectrum of each of the three components of each remaining window is then calculated using the Fast Fourier Transform (FFT), and the geometric mean of the amplitude spectral values of the horizontal components (N-S and E-W) are computed. The vertical and horizontal magnitude spectra are then smoothed using a filter with a 0.5 Hz width. Each window's horizontal amplitude spectrum is then divided by its vertical amplitude spectrum to calculate an HVSR for that window (26 total windows). The 26 HVSRs are then stacked and averaged to produce a single HVSR with the average spectral shape. The standard deviation of all of the windows' HVSRs is also calculated. The process of HVSR computations carried out by the MATLAB script is described in greater detail in Pontrelli (2020). The shapes of HVSR curves vary and can feature single or multiple peaks around a site's fundamental frequency as well as trough features that reach amplitudes below 1. Examples of such features are indicated in Figure 5.

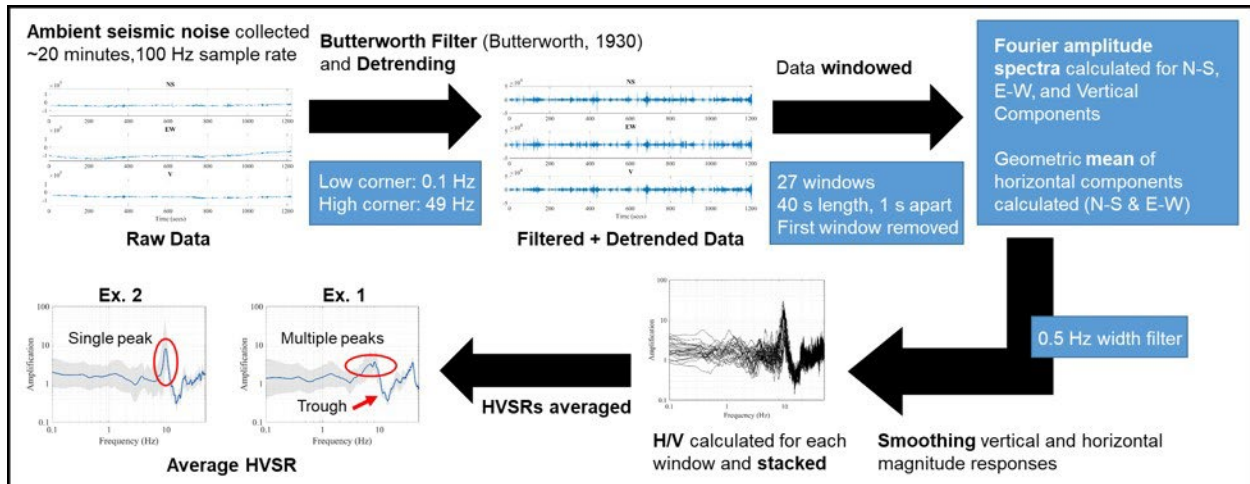


**Figure 5.** Flowchart illustrating the data processing and computation procedure used to calculate horizontal-to-vertical spectral ratios (HVSr). In the two provided examples of averaged HVSrs, a single fundamental resonance peak, multiple resonance peaks, and a trough are identified.

## Seismic Refraction Analysis

Seismic refraction analysis is used to estimate P-wave velocities and thicknesses of shallow subsurface soil layers. Seismic energy is generated from a “shot” source and propagates through the subsurface. When a seismic wave strikes a higher-velocity layer boundary at the critical angle, the wave is refracted laterally through the higher-velocity layer and then returns to the surface as a head wave (Kesarwani et al., 2012). The surface P-wave arrivals data are recorded on seismographs, and travel-time versus distance curves (T-X plots) are created. From a T-X plot, refractors are identified and layer P-wave velocities are estimated. From the measured P-wave arrival times and estimated velocities, the depths from the surface to each refractor can be calculated.

A series of seismic refraction measurements were performed at the Chestnut Hill Reservoir in June-August of 2022 in order to estimate seismic velocity profiles for the reservoir embankment. Refraction measurements were made at five locations along the top of the manmade embankment covering the area where ambient seismic noise data had been recorded to

produce HVSRs. Each measurement included 24 channels of seismic data collected from 4.5 Hz geophones. The geophones were placed in the soil atop the embankment (on the inner-slope side of the gravel path) and spaced 1.5 m from each other using a tape measure. Each line of 24 geophones extended a length of 34.5 m along the embankment. The approximate location of the midpoint of each was obtained using GPS. Figure 6 shows the locations of the geophone lines as well as a diagram of the measurement geometry. To collect the refraction data, seismic waves were generated by hitting a 15 lb sledgehammer on a steel plate at the ends of a line. Five shots were recorded at a shot offset of 7 m from the first geophone. This process was then repeated at the other end of the line to obtain refraction data from seismic waves coming from the opposite direction. The opposite ends of the lines are differentiated by “North Side” and “South Side.” Each measurement had a record length of 1 s and a sample rate of 2 ms.

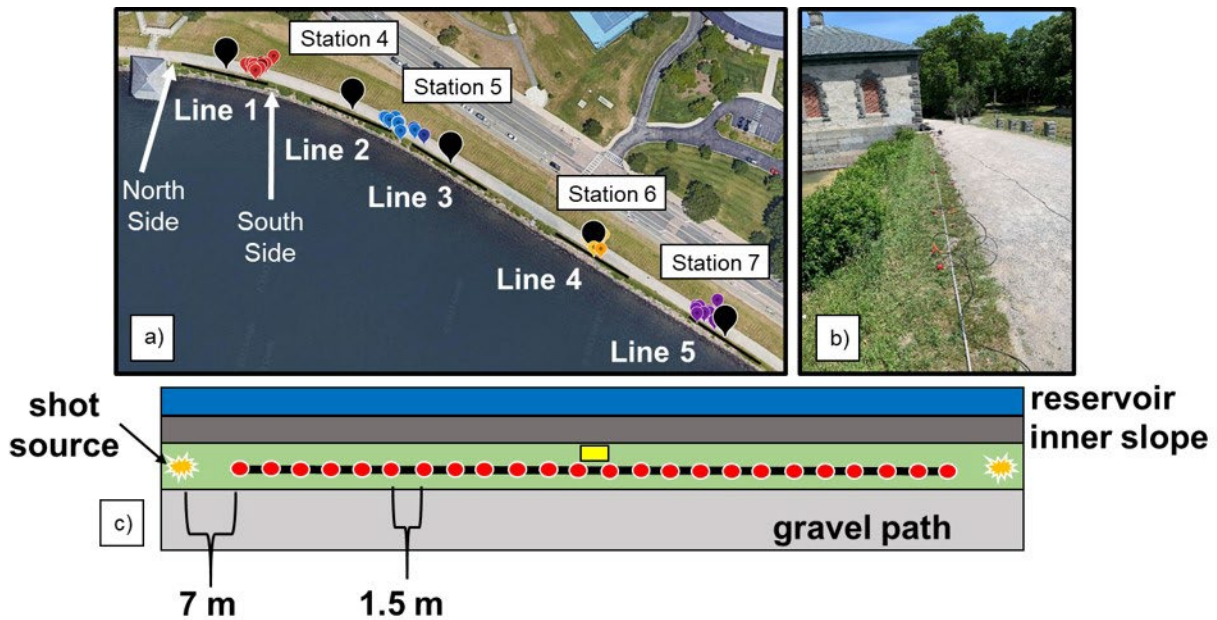


**Figure 6.** a) Map of all geophone line shot gathers (Lines 1-5) collected on the Chestnut Hill Reservoir embankment. The large black markers indicate the geophone line midpoints, and the north and south sides of Line 1 are indicated. The HVSR stations are plotted and labeled for reference. b) A picture of Line 1 North Side taken from atop the embankment. c) A bird's-eye view diagram of the geometry of a line. The central yellow box is the midpoint and the red circles represent geophone locations.

Three of the shot traces for each side of a geophone line were averaged before picking first P-wave arrival times. Although five sledgehammer shots were recorded from each side of a geophone line, only three of the five total shots for each measurement were averaged because the first P-wave arrivals of some shots were too indistinct to be discerned. The two shots with the most indistinct arrivals from each measurement were omitted from the analysis of the data. The poor arrivals were the result of several factors including varying shot strengths from the sledgehammer hits and varying amounts of manmade noise produced from people walking on the adjacent path or cars traveling along the road at the base of the embankment. T-X plots of time versus offset distance from the shot source like the one shown in Figure 7 were created from the averaged shot traces, and first P-wave arrival times were identified. In addition to manmade noise, natural noise and the decaying of seismic wave amplitudes due to geometric spreading and anelastic attenuation (Cormier, 1989) typically made it difficult to identify P-wave arrivals in channels farther from the shot source. First P-wave arrival times could only be identified accurately at channels within approximately 20-30 m from the shot source, and so only those channels could be analyzed for each T-X plot.

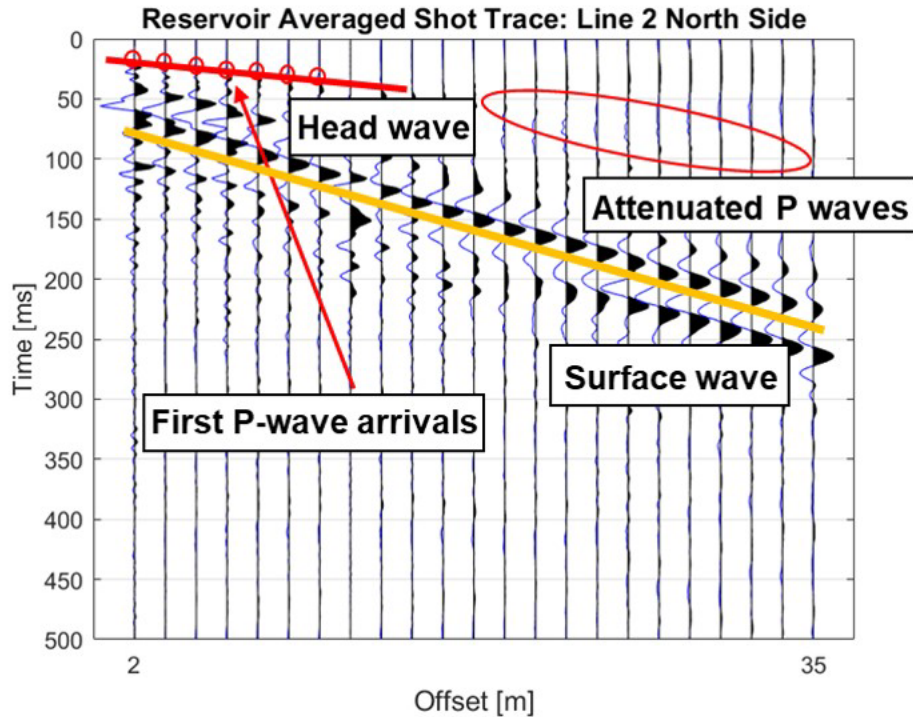


**Figure 7.** T-X plot (also known as a seismic section) of an averaged shot trace produced from geophone line shot gathers from Line 2 North Side on the Chestnut Hill Reservoir embankment. First P-wave arrivals (used in the refraction analysis) are circled in red and a head wave is identified by the red line. The attenuated P-wave amplitudes mixed with manmade and natural noise at farther offset distances are circled in red. The surface wave (used in MASW) is underlined in yellow.

In order to estimate wave velocities and layer thicknesses of the reservoir embankment, a series of calculations derived from Billen (2020) and Anomohanran (2013) were conducted from arrival time readings of the P wave for each seismic section. The first P-wave arrival times that could be identified in the T-X plots were used to identify refractors within the embankment. Different linear equations of the form  $f(x) = mx + b$ , where  $x$  is offset in meters,  $m$  is the slope of the line,  $b$  is the y-intercept, and  $f(x)$  is time in milliseconds, were fit to the different refractors observed in the T-X plot. The slopes of the equations represent the reciprocals of the P wave velocities ( $V_p$ ) of the refractors, thus:

$$V_{p_{refractor}} = \frac{1}{m_{refractor}} \cdot 1000 \quad \text{Eq. (2)}$$

The factor of 1000 in Eq. 2 is used to convert from velocity in m/ms to the desired m/s. Thus, P-wave velocity estimations could be calculated for each refracting layer identified in the T-X plot. Using the P-wave velocities and refractor slope values, estimations for the thicknesses of the refracting layers using the generalized depth equation derived in Anomohanran (2013) could be calculated as well:

$$h_i = \frac{(b_{i+1}/1000) \cdot V_{p_i} \cdot V_{p_{i+1}}}{2(V_{p_{i+1}}^2 - V_{p_i}^2)^{1/2}} \quad \text{Eq. (3)}$$

where  $h$  is refractor thickness in meters and subscripts denote the  $i^{th}$  refractor layer for which thickness is calculated with  $i + 1$  referring to the layer below the refractor. Furthermore, S-wave velocities ( $V_s$ ) for the refractors were estimated by scaling their P-wave velocities in order to create  $V_s$  profiles for the embankment. In less dense, unconsolidated sands and soils, P waves can be more than 2 times faster than S waves, but in dense, consolidated rock materials, P waves are less than 2 times faster (Lee, 2003). For modeling purposes, S-wave velocities for refractors expected to be soil layers in the embankment were estimated with a  $V_p$  to  $V_s$  ratio of 2. S-wave velocities for the bottom refractor, expected to be bedrock, were estimated using a  $V_p$  to  $V_s$  ratio of 1.73.

## **MASW**

Multi-Channel Analysis of Surface Waves (MASW) is a method used to estimate the shear-wave velocity profile of a site's subsurface using the dispersive properties of Rayleigh waves (Kesarwani et al., 2012; Park et al., 1998). To perform MASW, multi-channel shot gathers are first collected, dispersion curves are extracted from the surface-wave parts of each trace, and the dispersion curves are inverted to obtain  $V_s$  profiles. Unlike the seismic refraction method, one of the advantages of MASW is that it can identify low-velocity zones, and so it is complementary to a seismic refraction analysis when imaging a site's subsurface.

MASW was performed for the Chestnut Hill Reservoir embankment using the surface wave data (highlighted in Figure 7) from the same geophone line shot gathers that were used for the refraction analysis. The software used to perform MASW was the Surface module of Geogiga Seismic Pro by Geogiga Technology Corp., which is discussed in Liu (2017). Unlike the refraction analysis in which the traces were averaged, for each side of a geophone line (north and south sides), dispersion curves were extracted individually from the three traces with the highest-amplitude signals with the upper bounds of 300 m/s for phase velocity and 40 Hz for frequency (example shown in Figure 8). Inversions using the standard software settings were then run on each of the dispersion curves to estimate a  $V_s$  profile for each trace in a shot gather measurement. Additionally, recursive inversions in which successive  $V_s$  models resulting from dispersion curve inversions were used as the initial  $V_s$  models for further inversions were performed until the inversion code converged on an estimated velocity structure for the thickest part of the embankment.

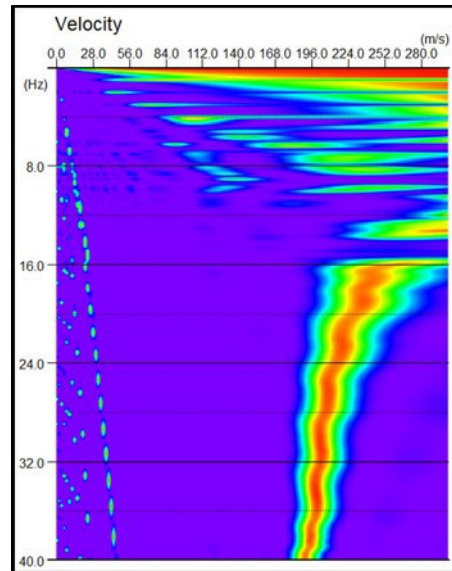


**Figure 8.** Dispersion curve produced by Geogiga Seismic Pro’s Surface Module. This dispersion curve was extracted from a seismic trace collected from the Line 2 North Side on the Chestnut Hill Reservoir embankment. Phase velocity ranges from 0 m/s to 300 m/s, and frequency ranges from 0 Hz to 40 Hz.

### HVSR Modeling

The program HV-Inv (García-Jerez et al., 2016) was used to estimate the seismic velocity structures of the Chestnut Hill Reservoir embankment and Franklin Falls Dam and to create theoretical HVSRs for the embankments. The purpose of estimating a seismic velocity structure for the embankments was to investigate the resolution at which the subsurface can be imaged by HVSR inversion and to compare the inversion results for the Chestnut Hill Reservoir embankment to those of the seismic refraction analysis and MASW performed as part of this research. Theoretical HVSRs were constructed for the embankment sites to investigate how well HVSRs calculated from ambient noise can be replicated by estimated seismic velocity structures for each site.

To obtain a subsurface seismic velocity profile for the Chestnut Hill embankment, an inversion was run on a Station 4 HVSR calculated from a normal water level measurement that is shown in Figure 9. Station 4 was selected as the target site for modeling because it is located on

the thickest part of the embankment where a structural integrity analysis might be desired. Furthermore, an HVSR from a normal water level measurement was chosen because the  $V_s$  profiles estimated from the refraction analysis and MASW were based on data collected when the water was near normal water level. To create a theoretical HVSR for Station 4 that most closely matches the observed HVSR, a single seismic velocity structure was constructed for the thickest part of the embankment through trial-and-error using the results of the various geophysical methods conducted at the reservoir embankment. This modeling process is illustrated in Figure 9.

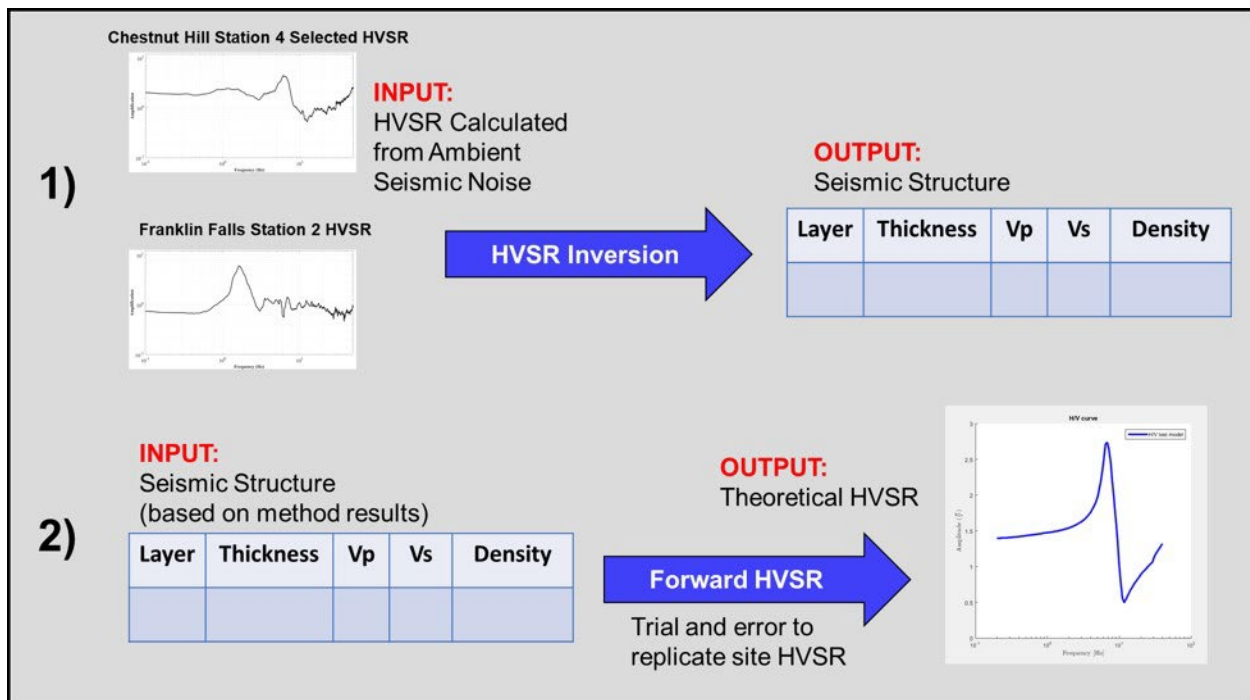


**Figure 9.** Flowchart of the modeling process performed in this study using HV-Inv. HVSRs calculated from ambient seismic noise measurements are first inverted by HV-Inv to estimate a seismic structure. Through a process of trial-and-error, the parameters of the seismic structure are changed based on the results of the other geophysical methods until a forward HVSR calculation yields a theoretical HVSR that closely matches the observed HVSR computed from the field data.

To estimate a subsurface seismic velocity structure for the Franklin Falls Dam, an inversion was run on the observed HVSR calculated for Franklin Falls Station 2 (hereby referred

to as FF Station 2) which is shown in Figure 9. The FF Station 2 HVSR was selected for inversion because it is located near the part of the dam with the thickest amount of built-up earthfill material (indicated by site fundamental frequency). A theoretical seismic velocity structure was then calculated through trial-and-error to produce a best-fit theoretical HVSR for FF Station 2.

## Results

### Chestnut Hill Reservoir Embankment

#### *HVSR*

The mean fundamental frequencies calculated from repeated HVSRs at the Chestnut Hill Reservoir embankment (Figure 10) range from 6.34 Hz at Station 4 where the embankment is thickest to 13.31 Hz at Station 8 where the embankment is thinnest. Depth to bedrock at each station (shown in Table 1) is calculated with these fundamental frequencies using Eq. 1 and assuming a sediment layer velocity of 210 m/s. A velocity of 210 m/s was chosen because the results of the seismic refraction analysis and MASW performed at the reservoir embankment (presented later) estimated a surface layer S-wave velocity of just over 200 m/s.

Station	Mean Fundamental Frequency (Hz)	Estimated Depth to Bedrock (m)
4	$6.34 \pm 0.22$	$8.28 \pm 0.29$
5	$7.66 \pm 0.69$	$6.85 \pm 0.62$
6	$10.78 \pm 0.17$	$4.87 \pm 0.08$
7	$9.79 \pm 0.12$	$5.36 \pm 0.07$
8	$13.31 \pm 0.86$	$3.94 \pm 0.25$

**Table 1.** The mean fundamental frequency and estimated depth to bedrock at each Chestnut Hill Reservoir embankment station. The depth to bedrock estimates were calculated using Eq. 1 and a surface layer velocity of 210 m/s. The standard deviation for a station's fundamental frequency determines the level of uncertainty of estimated depth to bedrock. Generally, depth to bedrock decreases in the south direction along the embankment from Station 4 to Station 8.

Depth to bedrock generally decreases toward the south from Station 4 (lower  $f_0$ ) to Station 8 (higher  $f_0$ ). The decrease in depth to bedrock corresponds with a decrease in embankment thickness to the south, and the calculations estimate that the bedrock must lie just below the bottom of the manmade embankment. The existence of bedrock just below the manmade embankment is also indicated by the bedrock outcroppings to the north of and within the reservoir.

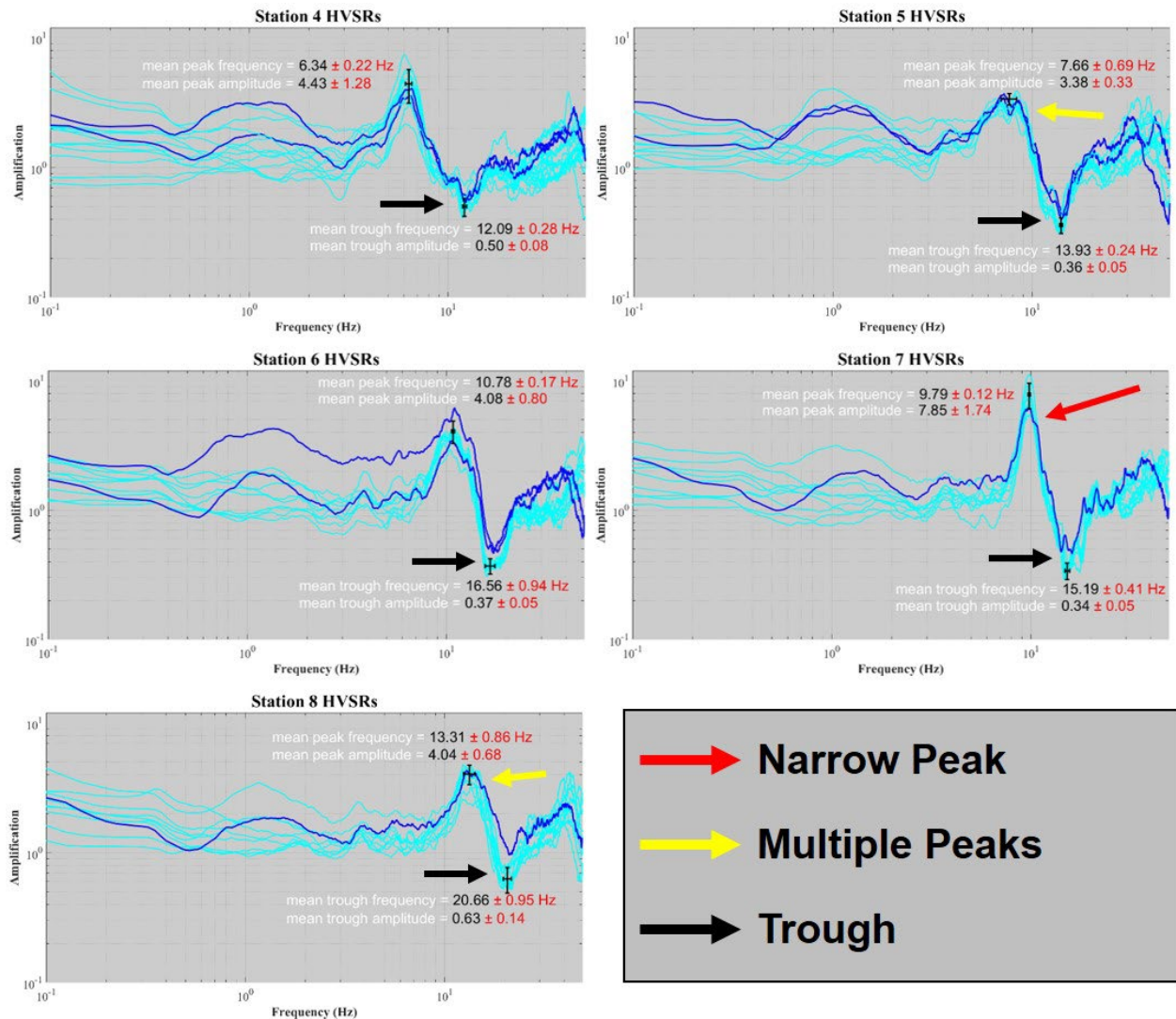


**Figure 10.** Repeated HVSR curves for Chestnut Hill Reservoir Stations 4-8. Mean fundamental peak frequencies and peak amplitudes are shown in black text with their respective standard deviations in red text (illustrated by error bars). The same information is shown for the trough frequencies and minimum spectral values. The light blue HVSRs are from normal reservoir water

level measurements (~131.5 ft) and the dark blue HVSRs are from low reservoir water level measurements (~125.5 ft). Arrows indicate various characteristics of the spectral ratios.

The uncertainties of the depth to bedrock calculations arise from variations in site fundamental frequency measured at different times and from the assumed 2-layer subsurface model. The standard deviation in fundamental frequency for each station is provided in Table 1 and illustrated in Figure 10. Stations 4, 6, and 7 have the lowest standard deviations in fundamental frequency and their HVSRs feature single prominent resonance peaks, whereas the fundamental frequencies of Stations 5 and 8, which have the highest standard deviations, feature multiple, closely-spaced resonance peaks that vary in prominence (Figure 10). Thus, the observed variability of fundamental frequency is higher for sites with wide or multiple resonance peaks than sites with narrow, single peaks. The 2-layer subsurface model used for depth to bedrock calculations assumes that the properties of the embankment subsurface are homogeneous down to the underlying bedrock boundary. Because the depth to bedrock estimate does not account for the effects of individual layers within the embankment, there is inherent uncertainty in choosing a single sediment layer velocity (such as 210 m/s assumed here) for the calculation. Further uncertainty is present due to the assumption that the bedrock layer is a single, flat surface. If the subsurface bedrock layer undulates or is a laterally uneven surface similar to the exposed bedrock outcroppings near the embankment, multiple reflections from bedrock might be observed in the HVSR.

The HVSRs of the Chestnut Hill Reservoir embankment stations all exhibited deep spectral troughs with amplitudes below 1.0 at frequencies about double those of their fundamental resonance peaks ( $2f_0$ ). Castellaro & Mulargia (2009) expect Rayleigh wave noise sources to be the causes of narrow HVSR troughs at frequencies of approximately  $2f_0$ . The

troughs occur approximately in the frequency range 11-21 Hz with corresponding peaks at 6-13 Hz. The mean standard deviation of trough frequency (measured at the deepest part of the trough) is 0.56 Hz, and the mean standard deviation of trough amplitude is 0.075. In most HVSRs, the spectral ratio value is 1.0 or greater because amplification of horizontal motion is typically greater than amplification of vertical motion (Tsai & Lui, 2017). However, even when uncertainty is taken into account, the troughs have a spectral ratio amplitude significantly below 1.0, indicating that vertical amplification is greater than horizontal amplification in the trough frequency bands. An interpretation of the cause of this trough is discussed later.

### ***Seismic Refraction Analysis***

From the seismic refraction analysis conducted as part of this thesis research, two or three refracting subsurface layers were identified at each geophone line across the reservoir embankment. The estimated depths of the refractors vary across Lines 1-5, but a surface layer with a thickness of about 1.3-3.3 m and an S-wave velocity of 175-290 m/s was identified in the Vs profiles of every line (Figure 11). Beneath this surface layer, the S-wave velocity was estimated to be roughly 400 m/s for a layer approximately 5-6 m-thick. A third layer was identified under Lines 2, 3, and 4 with its top at a depth of around 8-9 m. The estimated S-wave velocity for this layer ranged from about 675 m/s to 960 m/s. This deeper, high-speed layer is likely bedrock, which we assume to be just below the ground surface level on which the embankment is built. Thus, the results of the seismic refraction analysis estimate the depth to bedrock to be roughly 8-9 m under Lines 2, 3, and 4 on the embankment. Due to the attenuation of P waves on geophones with offset distances 30 m or farther from the shot source and the presence of noise, depths to bedrock under Lines 1 and 5 could not be identified. The depth to

bedrock under each line estimated by the seismic refraction analysis is provided in Table 2 as the average between the estimates from a line's north and south sides.

Line	Average Estimated Depth to Bedrock (m) - Seismic Refraction Analysis
1	N/A
2	8.5
3	8.5
4	8.2
5	N/A

**Table 2.** The average depth to bedrock under each geophone line estimated from the seismic refraction analysis performed at the Chestnut Hill Reservoir embankment. Due to high levels of noise, the bedrock layer depths were unable to be identified at Lines 1 and 5. The depth estimates are deeper than those from the HVSR and seismic refraction analyses.

## Chestnut Hill Reservoir Embankment Refraction Analysis Velocity Profiles

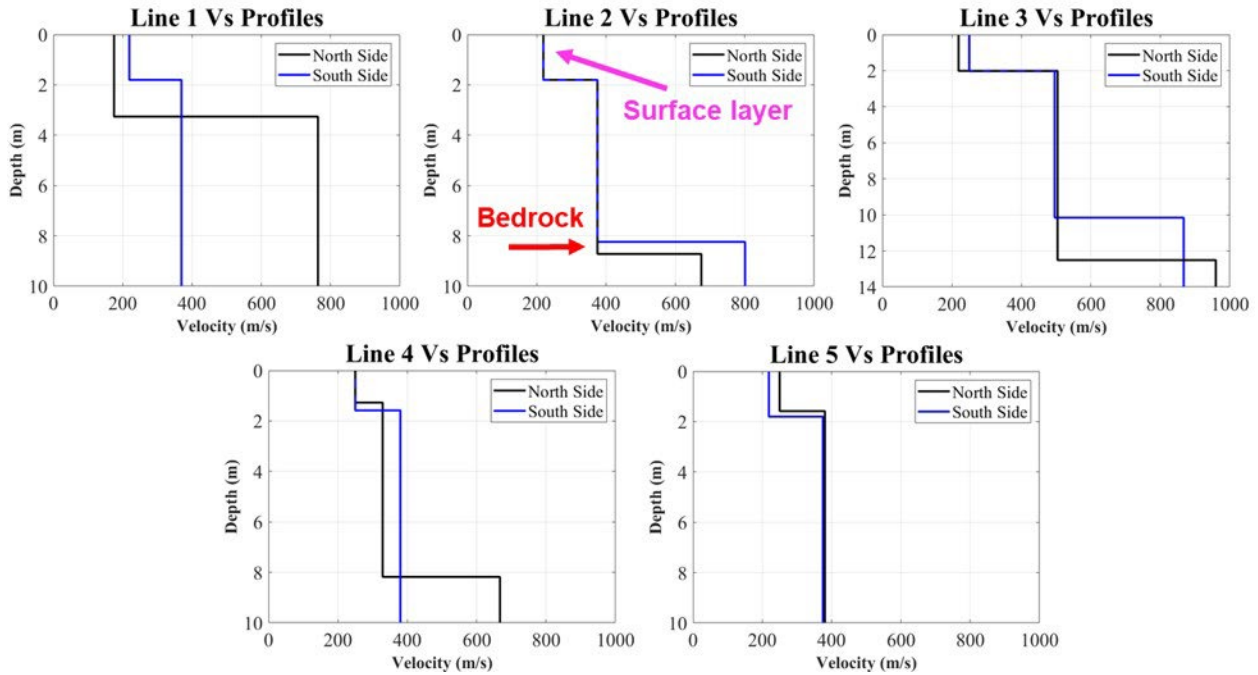


**Figure 11.** Shear-wave velocity profiles estimated by the seismic refraction analysis at all of the Chestnut Hill Reservoir embankment geophone lines. Surface layers with velocities between 200 m/s and 300 m/s with thicknesses of about 1-3 m were estimated at each line. In Lines 2-4, the bedrock layers were estimated to have depths of 8-9 m and velocities between 600 m/s and 1000 m/s. An example of a surface layer is indicated by the pink arrow in the Line 3 Vs profile, and an example of a bedrock layer is indicated by the red arrow in the same profile.

### *MASW*

Moving south along the embankment from Line 1 to 5, the average estimated depth to bedrock decreases from about 7.7 m to 5.8 m as the thickness of the embankment decreases. The average estimated depth to bedrock under each line is provided in Table 3 and the Vs profiles produced from the MASW analysis for Lines 1, 3, and 5 are displayed in Figure 12 to illustrate the change in bedrock depth along the embankment. The thicknesses and velocities of the subsurface layers above the estimated bedrock layer in the displayed Vs profiles are similar to each other. A surface layer with a thickness of about 2-3 m shows up in each of the Vs profiles with an S-wave velocity around 200 m/s. A thin, higher-velocity (~300 m/s) layer with a

thickness ranging from about 0.5-1 m is observed below the surface layer for all MASW lines and above a low-velocity zone comprised of multiple layers (often reaching a minimum velocity of less than 200 m/s) with a total thickness ranging from about 0.5-2.5 m. The high-velocity and low-velocity zones are indicated in Figure 12.

<b>Line</b>	<b>Average Estimated Depth to Bedrock (m) - MASW Inversion</b>	<b>Estimated Depth to Bedrock (m) - MASW Recursive Inversion</b>
1	7.7	7.8
2	8.0	6.5
3	6.9	N/A
4	5.9	N/A
5	5.8	N/A

**Table 3.** The average depth to bedrock under each geophone line estimated from the MASW method performed at the Chestnut Hill Reservoir embankment. Recursive inversions were run on the surface wave dispersion curves for Lines 1 and 2 because they are located on the thickest part of the embankment. Generally, depth to bedrock decreases in the south direction along the embankment from Line 1 to Line 5.

### Chestnut Hill Reservoir Embankment MASW Velocity Profiles

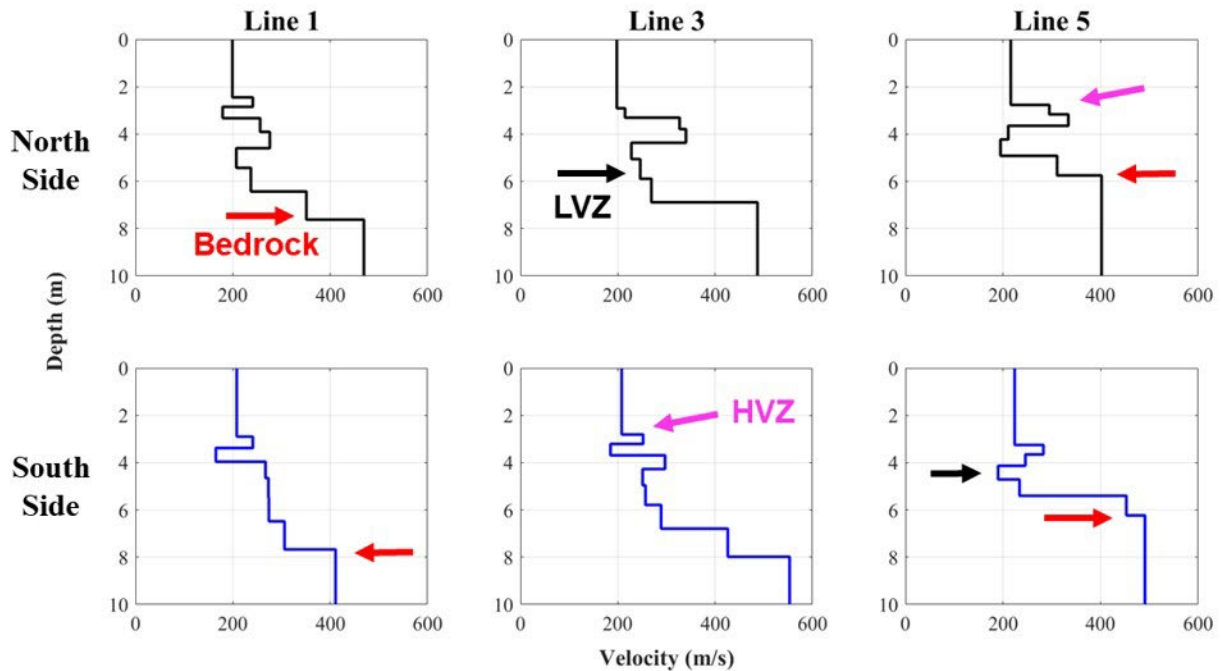


**Figure 12.** Shear-wave velocity profiles estimated by the MASW method for Lines 1-3 of the Chestnut Hill Reservoir embankment. A surface layer with a thickness of about 2-3 m and velocity of just over 200 m/s is estimated at each line. The bedrock layers, examples of which are indicated by the red arrows, have estimated velocities of about 400-500 m/s. A thin, high-velocity layer, indicated by the pink arrows, below the surface layer is observed in all of the Vs profiles immediately above an underlying low-velocity layer, indicated by the black arrows.

Recursive inversions of surface wave dispersion curves from the thickest part of the embankment converged on estimated Vs profiles (Figure 13), with each characterized by a thin, high-velocity layer with a thickness of about 0.5 m and a depth of approximately 2.5 m. A low-velocity zone lies immediately below the thin, high-velocity layer and is comprised of multiple layers with S-wave velocities within the range of 100-250 m/s. The thickness of the low-velocity zone (indicated in Figure 13) varies between the Vs profiles, but it is significantly thicker than the overlying high-velocity layer. The Vs profiles exhibit layers with higher velocity under the low-velocity zone. The depth to bedrock at Line 1 is estimated by the inversions to be about 7.8 m, which is similar to the average estimated depth from the single inversions for Line 1 (Table

3). However, the depth to bedrock at Line 2 is estimated to be about 6.5 m, which is shallower than the average estimate of 8.0 m from the single inversions for Line 2 (Table 3).

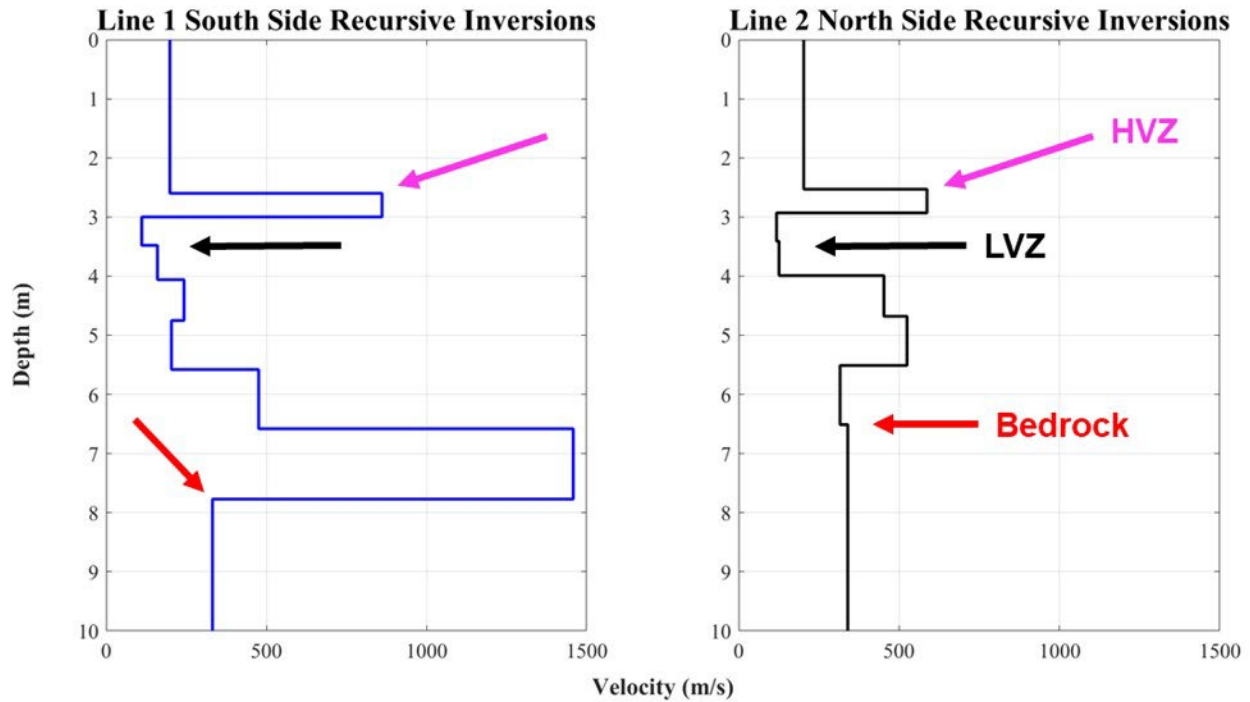


**Figure 13.** The shear-wave velocity profiles estimated by the MASW recursive inversions for Line 1 South Side and Line 2 North Side, which are located on the thickest parts of the Chestnut Hill Reservoir embankment near Station 4. The thin, high-velocity layers are indicated by pink arrows, the low-velocity zones immediately underlying the high-velocity zones are indicated by black arrows, and the estimated depths to bedrock are indicated by red arrows. The high-velocity zones have higher velocities than estimated by the initial MASW inversions. The low-velocity zones are significantly thicker than the overlying high-velocity zones.

### ***HVSR Inversion***

The subsurface seismic velocity structure produced from the HV-Inv inversion of an HVSR calculated for Station 4 at normal water level is provided in Table 4 and shown in Figure 14. The  $V_s$  profile exhibits a high-velocity (nearly 950 m/s) surface layer approximately 3.1 m-thick. Below the surface layer lies a low-velocity zone at a depth of 6 m with an S-wave velocity of about 326 m/s and a thickness of approximately 4.5 m. A layer with an S-wave velocity of

about 820 m/s lies immediately below the low-velocity zone, and the depth to bedrock is estimated to be nearly 13 m.

Layer	Thickness (m)	Vp (m/s)	Vs (m/s)	Density (kg/m <sup>3</sup> )
1	3.08	1936.26	947.18	2389.65
2	2.86	1705.88	919.32	2185.86
3	4.54	644.62	325.99	1162.90
4	2.47	1723.47	820.29	2029.75
5	0	2574.96	1248.21	2439.68

**Table 4.** The estimated Chestnut Hill Reservoir embankment subsurface seismic structure produced from the HV-Inv inversion of a Station 4 HVSR calculated from a normal water level seismic noise measurement. A high-velocity surface layer of about 950 m/s is estimated, and the estimated depth to bedrock is about 13 m.

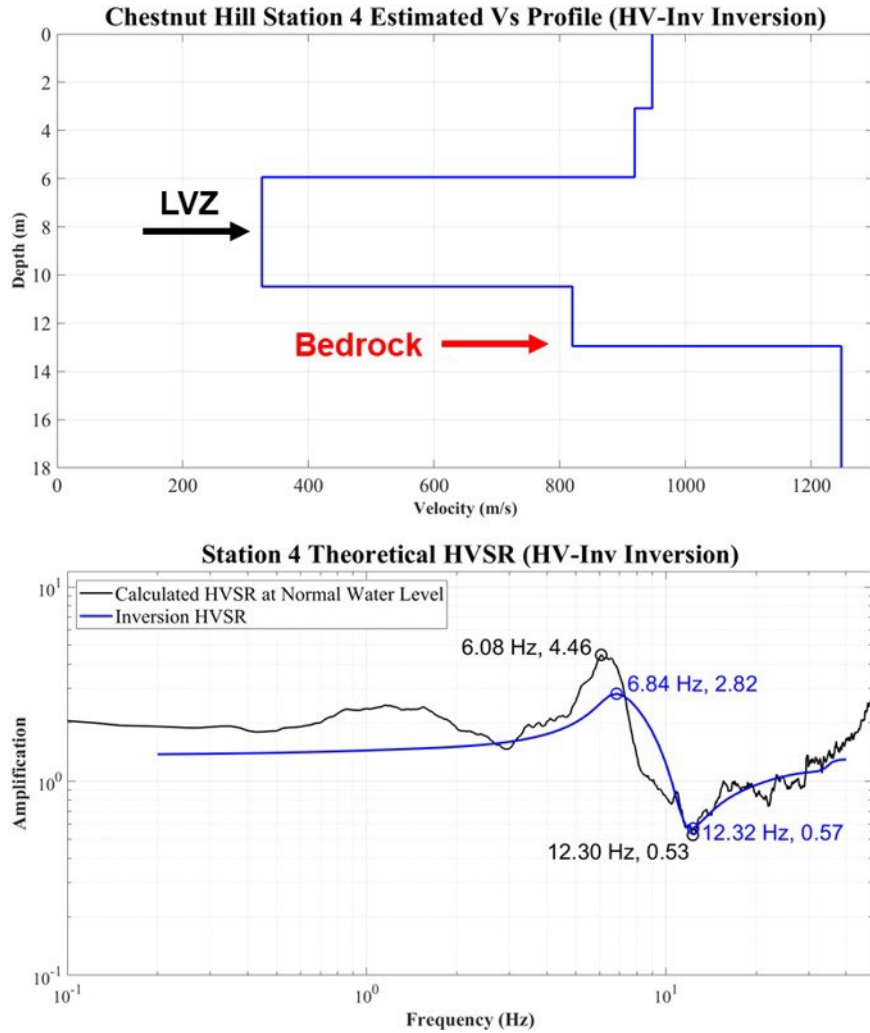


**Figure 14. (top)** The estimated shear-wave velocity profile for the Chestnut Hill Reservoir embankment produced from the HV-Inv inversion of a Station 4 HVSr. A low velocity zone with a depth of about 6 m and a thickness of about 4.5 m is indicated by the black arrow and has a speed of ~326 m/s. **(bottom)** The theoretical HVSr (blue) computed from the HV-Inv estimated seismic structure in Table 4. The Station 4 HVSr (black) on which the HV-Inv inversion was run is plotted for comparison. The fundamental frequency and trough of each HVSr is labeled.

The theoretical HVSr output from HV-Inv and the estimated seismic velocity structure from which it was computed are shown in Figure 14. In this figure, the theoretical HVSr is compared to the actual HVSr calculated for Station 4 on which the inversion was run. The fundamental frequency of the theoretical HVSr is 6.84 Hz, which is 0.76 Hz higher than the observed frequency of 6.08 Hz and more than one standard deviation away from the Station 4

average fundamental frequency of 6.34 Hz. The amplitude of the fundamental resonance peak of the theoretical HVSR is lower than that of the observed HVSR. The theoretical HVSR exhibits a trough with a minimum spectral value of 0.53 at 12.30 Hz that is very close in both frequency and amplitude to the trough of the observed HVSR.

### ***Summary of Methods and HVSR Modeling***

Of all of the geophysical methods employed to image the subsurface seismic velocity structure of the Chestnut Hill Reservoir embankment, the depth to bedrock estimates from the HVSR and MASW methods are most similar and are roughly within 1 m of each other. The depth estimates from the seismic refraction analysis are significantly higher for Stations 5 and 6 than those computed from the HVSR and MASW analyses. A comparison of the depth to bedrock estimates from each of the seismic data analysis methods is provided in Table 5. In general, the results indicate that depth to bedrock decreases moving south along the embankment from Station 4 to Station 8. The HVSR and MASW methods estimate bedrock to be at a depth just below the ground surface on which the embankment is built because the depth estimates at each station are similar to the height of the embankment at each station.

Station/Line	Embankment Thickness (m)	Estimated Depth to Bedrock (m)			
		HVSR	Seismic Refraction	MASW	HV-Inv Inversion
4 (Line 1)	6-7	8.3	-	7.7	13
5 (Lines 2 & 3)	5-6	6.9	8.5	8.0; 6.9	N/A
6 (Line 4)	4-5	4.9	8.5	5.9	N/A
7 (Line 5)	3-4	5.4	8.2	5.8	N/A
8	2-3	4.0	-	N/A	N/A

**Table 5.** The estimated depths to bedrock from each of the geophysical methods performed at the Chestnut Hill Reservoir embankment. Seismic refraction/MASW lines overlapping HVSR stations are grouped with those stations, and the approximate embankment thickness at each location is provided for comparison to bedrock depth.

The seismic velocity structures estimated from the MASW and the HV-Inv inversions suggest that there is at least one low-velocity zone within the Chestnut Hill Reservoir embankment. Figure 15 compares the Vs profiles constructed from the HV-Inv inversion of a Station 4 HVSR and of the recursive MASW inversions run on the surface wave dispersion curve collected from Line 2 North Side (located near Station 4). Although the velocities, depths, and thicknesses of the layers in the structures differ from one another, a high-velocity layer with an S-wave velocity somewhere in the range from 587 m/s to 947 m/s is estimated near the embankment surface. A low-velocity zone with a thickness between 1 m and 4.5 m appears immediately below this shallow, high-velocity layer. The S-wave velocities of the layers comprising the low-velocity zones range from 118 m/s to 326 m/s. The bedrock velocity varies greatly between the different Vs profiles and ranges from 340 m/s to 1248 m/s (Figure 15).

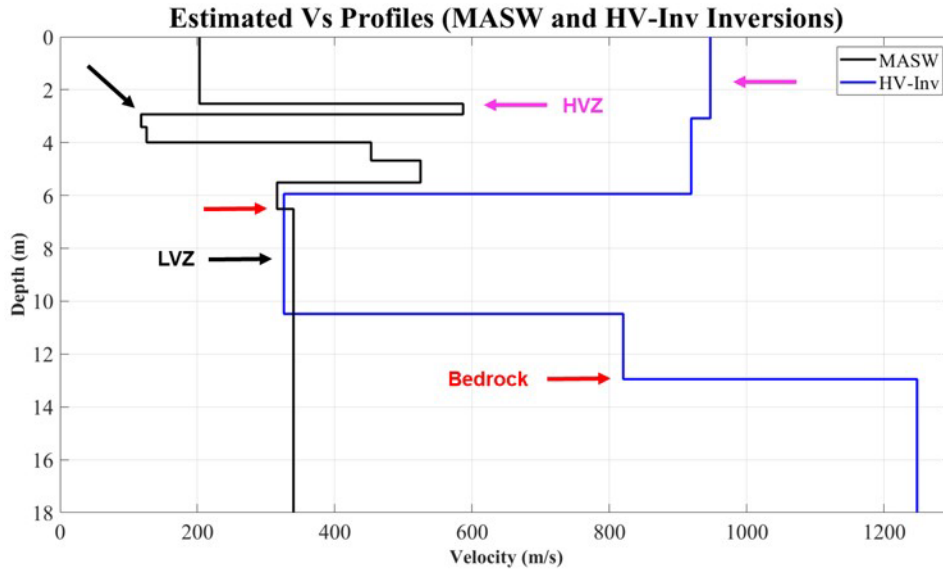


**Figure 15.** The shear-wave velocity profiles estimated from the MASW method (black) and HV-Inv inversion of a Station 4 HVSR (blue). Both Vs profiles have high-velocity layers at or near the surface (pink arrows) as well as low-velocity zones immediately underlying the high-velocity layers (black arrows). The estimated depths to bedrock (red arrows) between the two profiles differ by about 6.5 m.

Using the Vs profiles and depth to bedrock estimates from the various geophysical methods used in this thesis research, a single theoretical seismic velocity structure that is most consistent with the results of the different methods was constructed for Station 4 of the Chestnut Hill Reservoir embankment. The seismic velocity structure (provided in Table 6 and illustrated in Figure 16) features a 1 m-thick surface layer overlying a very thin, high-velocity layer near the surface of the embankment, which in turn overlies a 6 m-thick low-velocity zone comprised of two separate layers with slightly different S-wave velocities of 170 m/s and 200 m/s. Bedrock lies immediately beneath the low-velocity zone at a depth of 7.2 m and has an S-wave velocity of about 700 m/s.

Layer	Thickness (m)	Vp (m/s)	Vs (m/s)	Density (kg/m <sup>3</sup> )
1	1.00	400.00	200.00	2000.00
2	0.20	1557.00	900.00	2300.00
3	3.00	340.00	170.00	1000.00
4	3.00	400.00	200.00	1300.00
5	0	950.00	700.00	2000.00

**Table 6.** The theoretical seismic velocity structure proposed for Station 4 on the Chestnut Hill Reservoir embankment. A very thin, high-velocity layer immediately underlies the surface layer. A low-velocity zone immediately underlies the high-velocity layer. The bedrock layer is estimated to have a shear-wave velocity of about 700 m/s and a depth of just over 7 m.

The best-fit theoretical HVSR produced by HV-Inv from this seismic velocity structure is shown in Figure 16. The fundamental frequency (6.48 Hz) of the theoretical HVSR is within one standard deviation of the observed mean fundamental frequency of Station 4 (6.34 Hz). The amplitude of the fundamental resonance peak (4.41) is also within one standard deviation of the observed mean peak amplitude (4.43) at Station 4. The theoretical HVSR exhibits a deep trough with an amplitude well-below 1.0 at a frequency of 11.07 Hz, which is just more than one standard deviation away from the observed mean trough frequency (12.09 Hz).

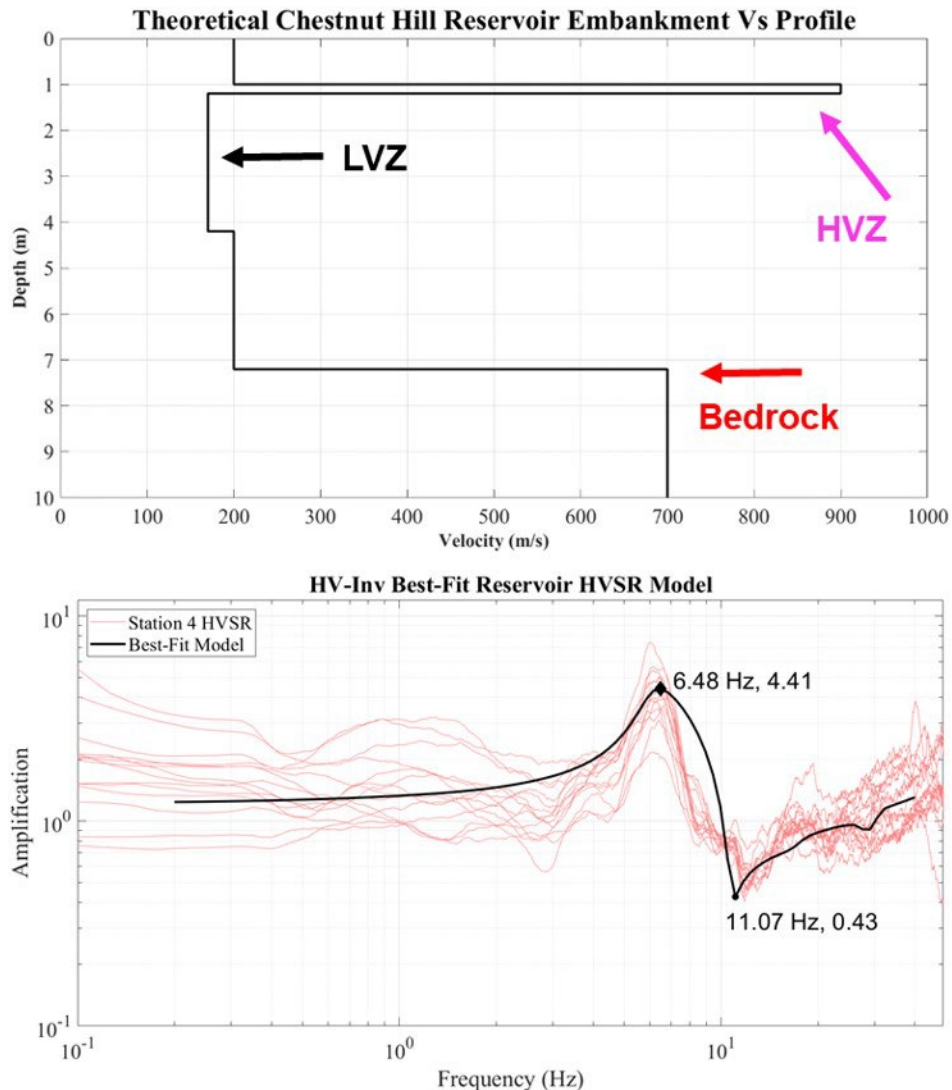


**Figure 16. (top)** The estimated theoretical shear-wave velocity profile for Station 4 on the Chestnut Hill Reservoir embankment was based on the results of all the geophysical methods performed at the embankment. The very thin, high-velocity zone is indicated by a pink arrow and the relatively thicker low-velocity zone is indicated by a black arrow. The bedrock layer is indicated by a red arrow. **(bottom)** The best-fit theoretical HVSR (black) computed by HV-Inv from the theoretical seismic velocity structure in Table 6. The fundamental frequency and minimum trough spectral values are circled and provided. All HVSRs calculated for Station 4 (red) are plotted for comparison with accompanying error bars showing the variations of fundamental frequency and trough spectral values.

## Franklin Falls Dam

### *HVSR*

The fundamental frequencies observed from the single set of HVSRs calculated for the Franklin Falls Dam range from 1.63 Hz at Station 1 to 11.5 Hz at Station 11. Depth to bedrock at each station (shown in Table 7) is calculated with these fundamental frequencies using Eq. 1 and assuming a sediment layer velocity of 210 m/s (the same velocity used for the Chestnut Hill Reservoir embankment calculations).

FF Station	Fundamental Frequency (Hz)	Estimated Depth to Bedrock (m)
1	1.63	32.21
2	1.65	31.82
3	1.85	28.38
4	2.10	25.00
5	2.08	25.24
6	2.38	22.06
7	2.50	21.00
8	2.67	19.66
9	4.08	12.87
10	4.25	12.35
11	11.5	4.57

**Table 7.** The fundamental frequency and estimated depth to bedrock at each Franklin Falls Dam station. The depth to bedrock estimates were calculated using Eq. 1 and a surface layer velocity of 210 m/s. Generally, the depth to bedrock decreases in the southwest direction along the dam from FF Station 1 to FF Station 11.

Depth to bedrock generally decreases moving southwest from Station 1 (lower  $f_0$ ) to Station 11 (higher  $f_0$ ). The dam is approximately uniform in height (~43 m) above the water surface of the Pemigewasset River, but the depth to bedrock calculations indicate that the earthfill material

within the embankment is not of uniform thickness, as there must be a greater amount of earthfill built-up on the northeast side of the dam, where presumably there is a greater depth to bedrock than on the southwest side.

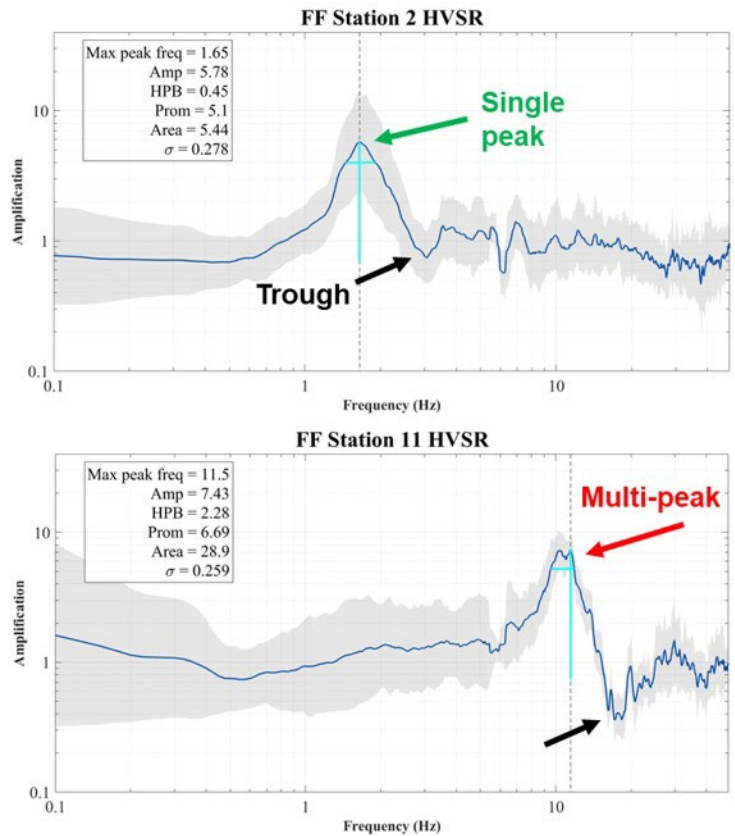


**Figure 17.** Examples of the HVSrs calculated for the Franklin Falls Dam. FF Station 2 (top) has a lower fundamental frequency than FF Station 11 (bottom), suggesting that the depth to bedrock at FF Station 2 is deeper than at FF Station 11. FF Station 2 has a single fundamental resonance peak (pink arrow), FF Station 11 has multiple closely-spaced peaks near its fundamental frequency (red arrow), and both HVSrs have troughs with spectral values below 1.0 (black arrows).

Although the temporal variability of fundamental frequency cannot be quantified for the spectral ratios of the Franklin Falls Dam since only one set of measurements was made, uncertainty trends can be estimated by comparing the shapes of the spectral curves calculated for the Franklin Falls Dam to those of the Chestnut Hill Reservoir embankment. Fundamental frequencies vary the most for Chestnut Hill Reservoir embankment spectral curves that feature multiple, closely-spaced resonance peaks with varying prominence. Several of the HVSrs

calculated for the Franklin Falls Dam (examples of which are shown in Figure 17) have wide or multiple resonance peaks, and so the fundamental frequencies at those stations are likely more variable than at stations with single, narrow peaks. Uncertainties of the depth to bedrock calculations for the Franklin Falls Dam also include the assumed 2-layer model of a homogeneous sediment layer overlying a flat bedrock layer and the assumption of the same sediment layer velocity (210 m/s) used for the bedrock depth estimates for the Chestnut Hill Reservoir embankment. The same sediment layer velocity was used because no other geophysical methods were employed at the Franklin Falls Dam to estimate its seismic velocity structure.

### ***HVSR Inversion and Modeling***

The subsurface seismic velocity structure estimated from the HV-Inv inversion of the calculated FF Station 2 HVSR is provided in Table 8 and illustrated in Figure 18. The  $V_s$  profile contains a nearly 34 m-thick surface layer with an S-wave velocity of just over 500 m/s. Immediately beneath this surface layer is a low-velocity layer with an S-wave velocity of about 350 m/s and a thickness of about 21 m. Bedrock is estimated to have a high S-wave velocity (roughly 1850 m/s) relative to the overlying layers, and the depth to bedrock is estimated to be approximately 55 m.

Layer	Thickness (m)	Vp (m/s)	Vs (m/s)	Density (kg/m <sup>3</sup> )
1	33.74	1206.16	516.07	1900.02
2	20.82	634.15	356.37	2004.49
3	0	3341.25	1855.15	1034.27

**Table 8.** The estimated Franklin Falls Dam subsurface seismic structure produced from the HV-Inv inversion of the FF Station 2 HVSr. A low-velocity zone is estimated at a depth of about 34 m, and the depth to bedrock is estimated to be about 55 m.

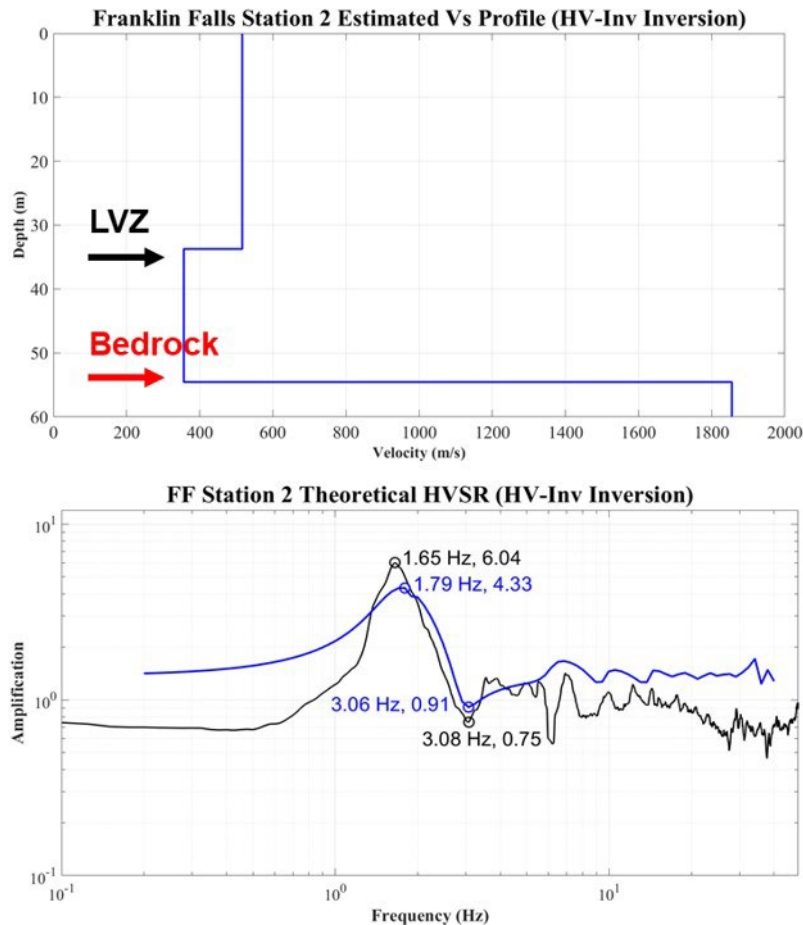


**Figure 18. (top)** The estimated shear-wave velocity profile for the Franklin Falls Dam produced from the HV-Inv inversion of the FF Station 2 HVSr. A low velocity zone at a depth of about 34 m is indicated with a black arrow and has a speed of ~356 m/s. The depth to bedrock is estimated to be about 55 m and is indicated with a red arrow. **(bottom)** The theoretical HVSr (blue) computed from the HV-Inv estimated seismic structure in Table 8. The FF Station 2 HVSr (black) on which the HV-Inv inversion was run is plotted for comparison. The fundamental frequency and trough of each HVSr is labeled.

The theoretical HVSR output from HV-Inv and the FF Station 2 estimated seismic velocity structure from which it was computed are shown in Figure 18. In this figure, the theoretical HVSR is compared to the actual HVSR calculated for FF Station 2 on which the inversion was run. The fundamental frequency of the theoretical HVSR is 1.79 Hz, which is 0.14 Hz higher than the observed frequency of 6.04 Hz. The amplitude of the fundamental resonance peak of the theoretical HVSR is lower than that of the observed HVSR. The theoretical HVSR exhibits a trough with a minimum spectral value of 0.91 at 3.06 Hz that is very close in frequency to the trough of the observed HVSR.

A theoretical seismic velocity structure was constructed for FF Station 2 of the Franklin Falls Dam based on the depth to bedrock estimations from the HVSR method and HV-Inv inversion results. The seismic velocity structure (provided in Table 9 and illustrated in Figure 19) features a surface layer with a thickness of 30 m and an S-wave velocity of 500 m/s. A low-velocity layer with an S-wave velocity of 250 m/s lies immediately beneath the surface layer and has a thickness of 15 m. The bedrock layer is estimated to have an S-wave velocity of 1400 m/s and a depth of 45 m.

Layer	Thickness (m)	Vp (m/s)	Vs (m/s)	Density (kg/m <sup>3</sup> )
1	30.00	800.00	500.00	2000.00
2	15.00	500.00	250.00	1700.00
3	0	2422.00	1400.00	2500.00

**Table 9.** The theoretical seismic velocity structure proposed for FF Station 2 on the Franklin Falls Dam. A 30 m-thick surface layer overlies a low-velocity layer. The bedrock layer is estimated to have a shear-wave velocity of about 1400 m/s and a depth of 45 m.

The best-fit theoretical HVSR produced by HV-Inv from the seismic velocity structure of Table 9 is shown in Figure 19. The fundamental frequency (1.61 Hz) and amplitude of the

fundamental resonance peak (6.07) of the theoretical HVSR are both very close to those observed at FF Station 2 (1.65 Hz and 6.04, respectively). The trough of the best-fit theoretical HVSR has a minimum spectral value of 0.71, which is similar to the minimum value of the observed trough and close in frequency as well.

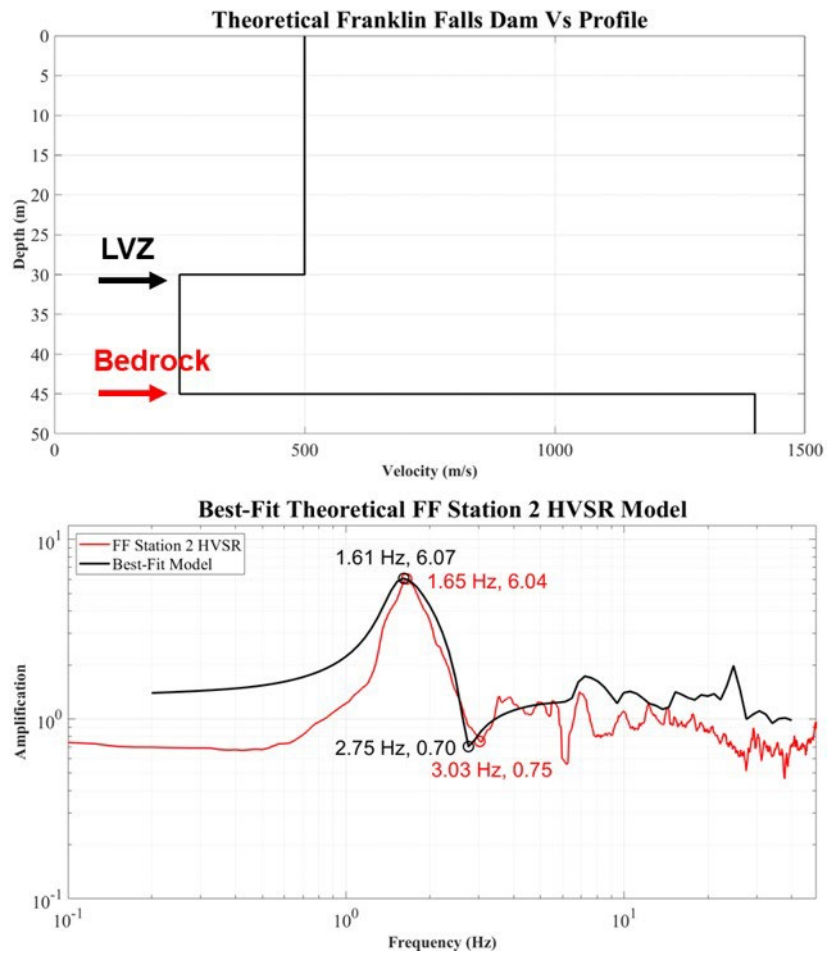


**Figure 19. (top)** The estimated theoretical shear-wave velocity profile for FF Station 2 on the Franklin Falls Dam. The seismic structure was estimated through a process of trial-and-error to replicate the observed HVSR for FF Station 2. The estimated low-velocity zone is indicated by a black arrow, and the bedrock layer is indicated with a red arrow. **(bottom)** The best-fit theoretical HVSR (black) computed by HV-Inv from the theoretical seismic velocity structure in Table 9. The fundamental frequency and minimum trough spectral values are circled and provided.

## **Effect of Water Level on HVSRs**

The average spectral ratio of all the observed HVSRs at normal water level (131.6 ft) for each Chestnut Hill Reservoir embankment station was calculated. For each station, the average spectral ratio at normal water level is compared to the spectral ratio at low water level (125.5 ft) in Figure 20. Since only one or two HVSRs per station were calculated when the reservoir was at low water level, the pictured low water level spectral ratios are either the average of the two observed HVSRs for a station or just the single observed HVSR.

The fundamental resonance peaks of each station's spectral ratios closely align near the same frequency, and so fundamental frequency does not vary significantly between the measurements at the different water levels recorded at the Chestnut Hill Reservoir. The spectral ratios of each station are also similar in shape. For example, both water level HVSRs of Station 5 exhibit two closely-spaced fundamental resonance peaks with similar prominence, whereas the spectral ratios of Station 7 both have narrow fundamental resonance peaks with high amplitudes relative to the resonance peaks at other stations.

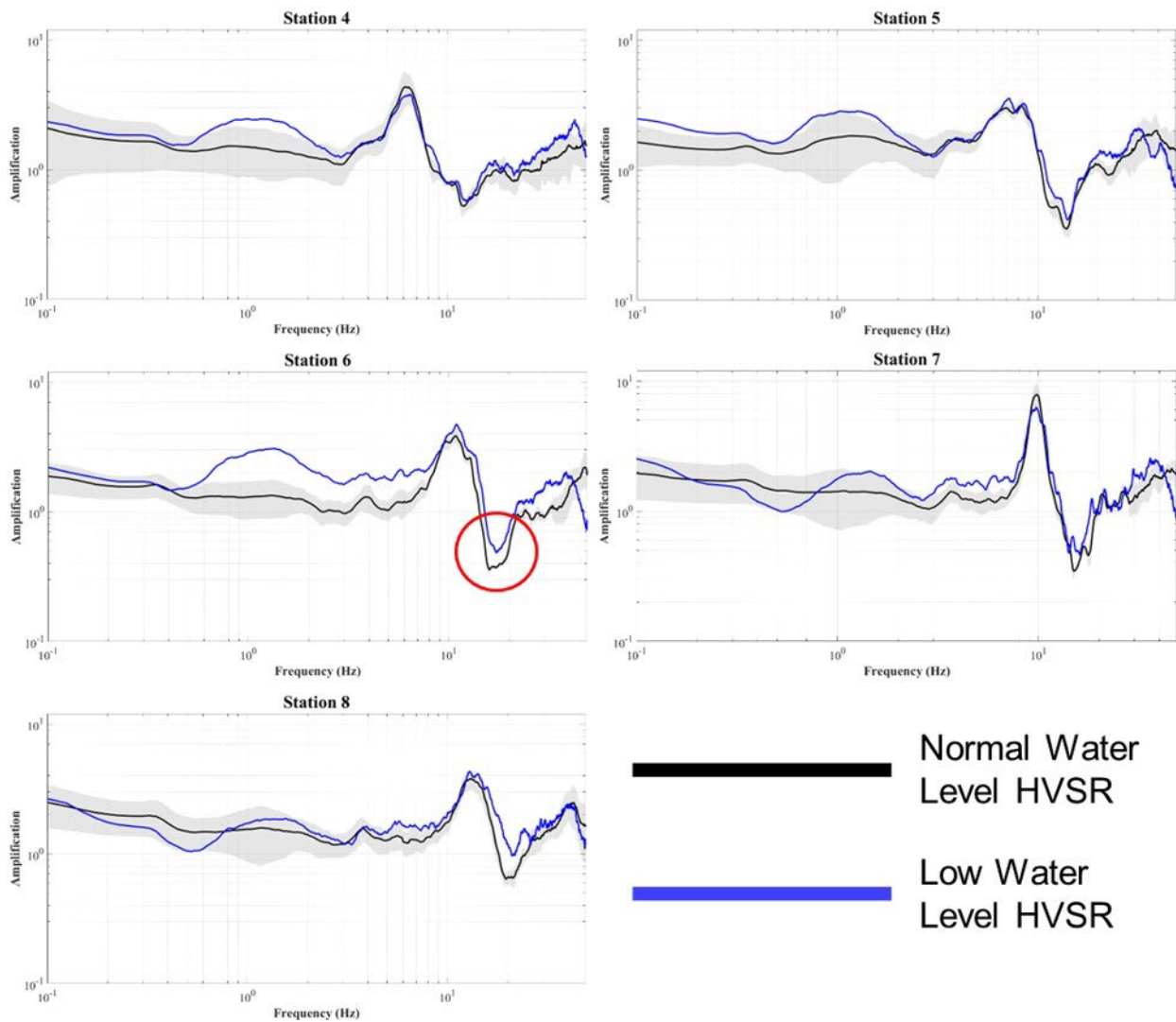


**Figure 20.** The average HVSR from seismic noise measurements made when the reservoir was at water levels near 131.5 ft (normal water level) is plotted in black for each station on the Chestnut Hill Reservoir embankment with standard deviation bounds drawn in gray. The blue HVSRs are the average spectral ratios from noise measurements at about 125.5 ft (low water level). Fundamental frequency does not vary significantly with water level, but the spectral values of the troughs in low water level HVSRs were more than one standard deviation higher than in normal water level HVSRs for Stations 5-8. An example of a difference in trough spectral values is circled in red.

The minimum amplitudes of the spectral troughs discussed earlier of the low water level HVSRs are consistently higher (the troughs are more shallow) than those of the normal water level HVSRs. At Stations 5-8, the minimum trough spectral values of the low water level HVSRs are more than one standard deviation higher than those of the normal water level HVSRs. The

frequencies at which the troughs occur, however, do not appear to vary as a function of reservoir water level. The observed minimum amplitudes of the trough features of all calculated HVSRs are plotted against reservoir water level in Figure 21. The strength of the linear relationship, measured by coefficient of determination ( $r^2$ ) values, between trough amplitude and water level varies between stations from low correlations at Stations 4 and 5 to moderate correlations at Stations 6-8.

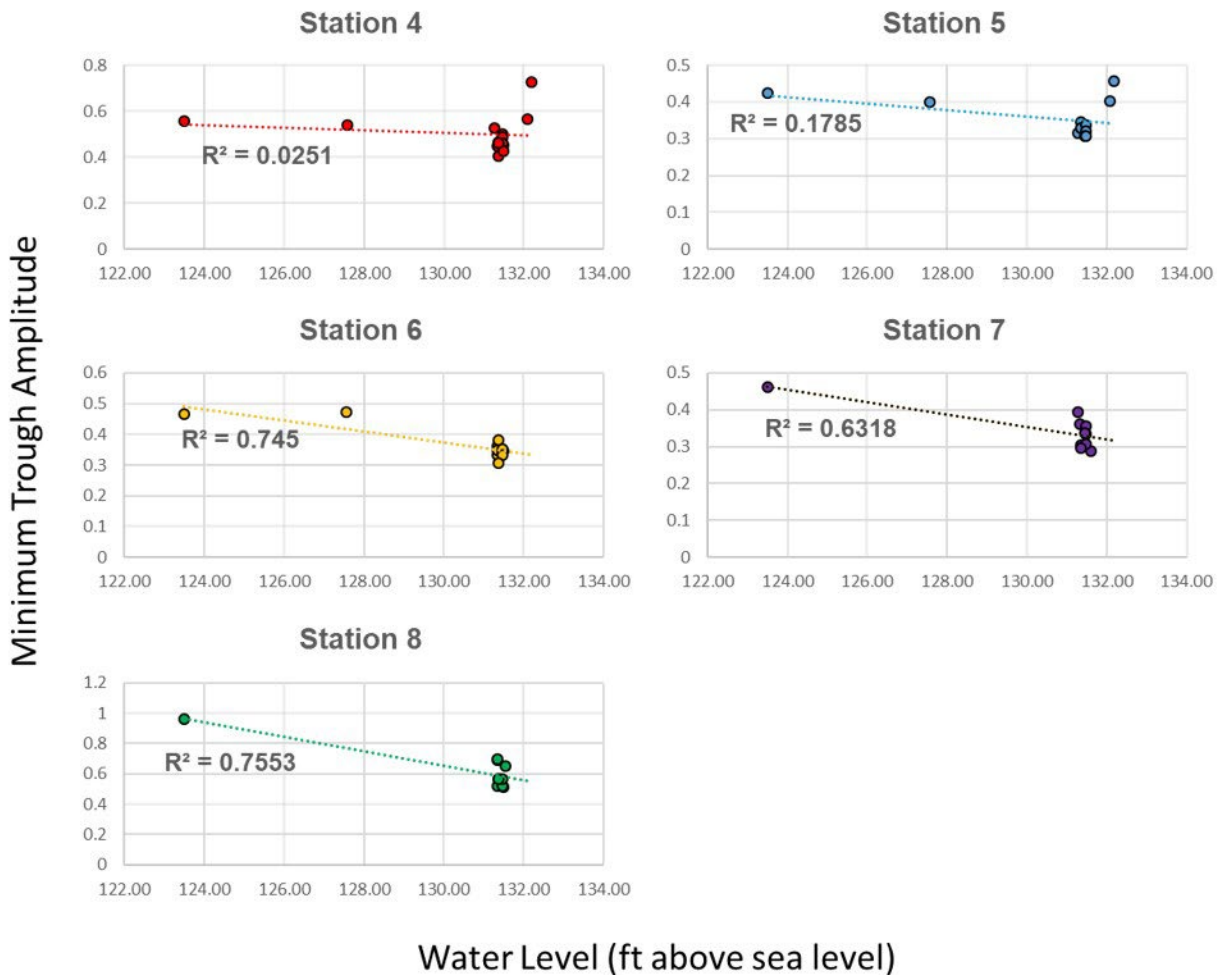


**Figure 21.** Scatter plots of minimum trough amplitude as a function of water level for each of the Chestnut Hill Reservoir embankment stations. The plots are fit with linear trend lines and the coefficient of determination ( $r^2$ ) value is shown to quantify the strength of the linear relationship between minimum trough spectral value and reservoir water level.

To investigate which changes in seismic structure could increase the spectral values of a trough within an HVSR, velocities in the theoretical seismic structure estimated for the Chestnut Hill Reservoir embankment (Table 6) were varied. Decreasing the P and S-wave velocities of the thin, high-velocity layer by 20% caused the amplitude of the trough to increase from the original value, and no change in fundamental frequency was observed. Additionally, increasing the P and S-wave velocities of the low-velocity layer immediately underlying the high-velocity layer by 20% caused an increase in trough amplitude from the original value as well as an increase in fundamental frequency by 0.36 Hz. The HVSR models resulting from these velocity changes are shown in Figure 22.

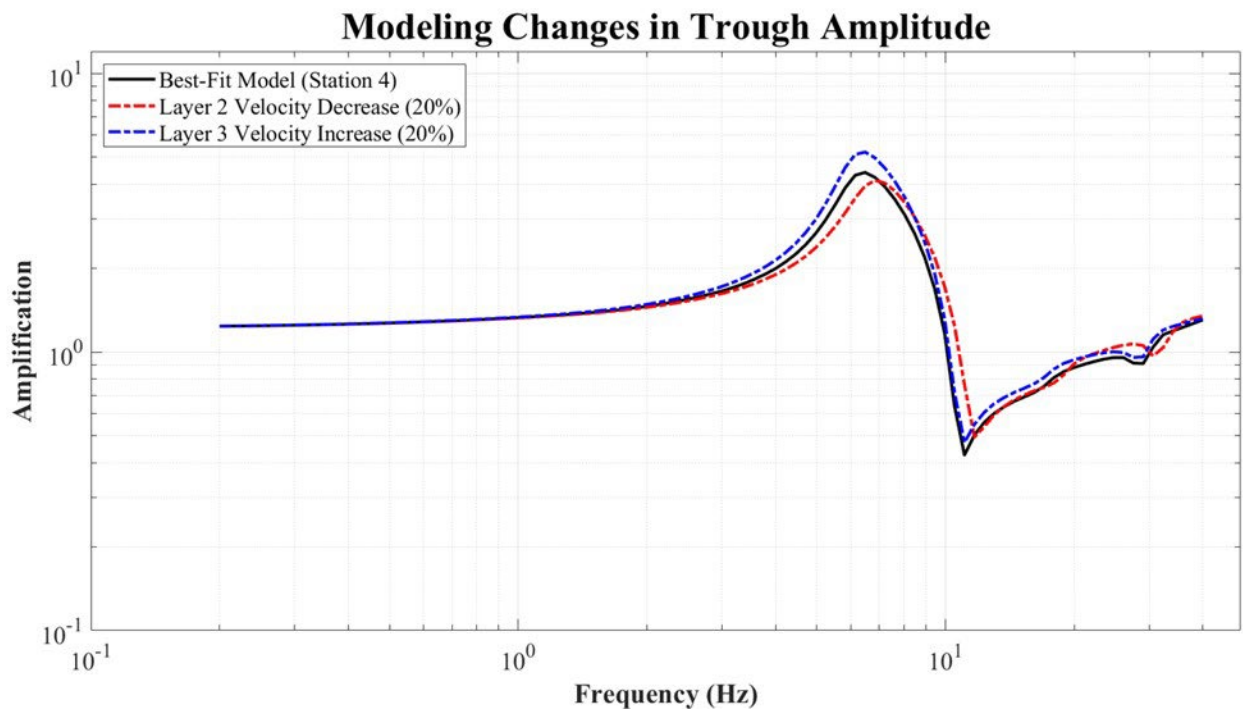


**Figure 22.** The best-fit HVSR (computed in HV-Inv from the theoretical seismic structure in Table 6) for Station 4 on the Chestnut Hill Reservoir embankment is shown in black. Increased minimum spectral values of the model’s trough are observed from decreasing the velocity of both P and S waves of the thin, high-velocity layer (layer 2) within the seismic structure by 20% as well as from increasing the velocity of the low-velocity layer (layer 3) by 20%. The resulting HVSR models are shown in red and blue, respectively.

## Discussion

The combination of results from the HVSR method, seismic refraction analysis, and MASW conducted at the Chestnut Hill Reservoir were used to estimate a subsurface seismic structure (Table 6) for the thickest part of the reservoir embankment. The seismic structure produced a theoretical HVSR that closely matches the observed HVSRs. The depth to bedrock estimates from MASW and the fundamental frequencies obtained from the HVSR method were similar at all sites where both ambient seismic noise and seismic refraction/MASW data were collected, varying by about 1 m or less. However, the depth to bedrock estimated from the seismic refraction analysis was deeper (by up to 3 m at some sites) than the depth estimated from HVSR and MASW, and the S-wave velocity estimates from the seismic refraction analysis were faster in general, although this could be an artifact of the P-to-S velocity conversion that was used. The results of the seismic refraction analysis and MASW were very similar at shallow depths. The methods both estimated a surface layer thickness of about 1.5-2.5 m and an S-wave velocity of just over 200 m/s.

The estimated seismic velocity structures from the MASW and HV-Inv inversions conducted for the Chestnut Hill Reservoir embankment contain low-velocity zones immediately beneath a thin high-velocity layer. The high-velocity layer could be a hard, high-density material (such as rock) used to reinforce the embankment near its crest, and such a layer is diagrammed in Figure 3. Furthermore, a low-velocity zone within the reservoir embankment could explain the deeper depth to bedrock estimates from the seismic refraction analysis relative to those from the MASW. When the velocity of a subsurface layer is lower than that of the overlying layer, the low-velocity layer cannot be identified in the T-X plot, which results in an overestimate of the thickness of the overlying layer as well as the depths of deeper, underlying layers (Sain &

Reddy, 1995). Thus, assuming a low-velocity zone exists within the embankment, the deeper depth to bedrock estimates from the seismic refraction analysis relative to the other methods are likely the results of overestimations. Furthermore, the theoretical HVSRs modeled by HV-Inv inversions only contain troughs with minimum spectral values below 1.0 when the inversion allows for low-velocity zones to exist in the estimated seismic structure regardless of the number of Rayleigh modes included in the direct HVSR calculation (which the user can input). Taking into consideration Castellaro & Mulargia (2009), who found that spectral values below 1.0 over a wide frequency band within an HVSR are indicative of low-velocity zones at a site, the troughs observed in the Chestnut Hill Reservoir embankment HVSRs might offer examples of sufficiently wide frequency bands that indicate low-velocity zones.

The results of the conducted seismic refraction analysis and MASW at the Chestnut Hill Reservoir support the HVSR method as an effective tool for estimating the depth to bedrock from the top of an earth embankment levee or dam. With a measured value for the surface layer S-wave velocity, many other studies such as (Simms et al., 2022) have also determined that the HVSR method is effective for estimating the depth to bedrock at an earth embankment. Thus, the HVSR method is most effective at estimating subsurface seismic structure when used in conjunction with other methods that can estimate layer velocities such as seismic refraction analysis or MASW. The MASW performed at the Chestnut Hill Reservoir embankment in this study was particularly effective as a complement to the HVSR method because it estimated the deeper layers of the embankment's seismic structure with greater resolution than the seismic refraction analysis. The seismic refraction analysis at the public Chestnut Hill Reservoir embankment was hindered in part by the noise and low source energy, which made it difficult to discern first P-wave arrivals at offsets farther than 30 m from the shot source. MASW was also

determined to have greater resolution than seismic refraction analysis at sites with high levels of industrial noise in Gorstein & Ezersky (2015).

The depth to bedrock estimated using the observed fundamental frequency at Franklin Falls Station 2 and an average S-wave velocity of the dam of 210 m/s is about 13 m shallower than the depth used in the theoretical seismic structure in Table 9 to replicate the station's observed HVSR. Because no other methods were employed at the Franklin Falls Dam to estimate layer thicknesses or velocities of the subsurface structure, it is not possible to independently confirm the estimated depths to bedrock found in this study using the HVSR data. It is possible that the discrepancy between the estimated depths is due to the assumed surface layer S-wave velocity of 210 m/s that was used in Eq. 1 when estimating the depth to bedrock based on the site's observed fundamental frequency. Performing this same calculation using a faster layer velocity and the same fundamental frequency would yield a deeper estimated value of the depth to bedrock. The surface layer S-wave velocity of the theoretical seismic velocity structure is 500 m/s, and so the average S-wave velocity of the dam's surface layer is likely closer to 500 m/s than to 200 m/s.

Observed site fundamental frequency did not vary significantly with changes in the water level of the Chestnut Hill Reservoir. However, the minimum spectral value of the trough of the low water level HVSR was more than one standard deviation higher than that of the normal water level HVSR for reservoir embankment stations 5-8 (shown in Figure 20). The modeling results displayed in Figure 22 indicate that a decrease in seismic velocity of the thin, high-velocity layer and/or an increase in the velocity of the underlying low-velocity layer causes an increase in the spectral value of the trough in the theoretical HVSR relative to its original value. The causes of such velocity changes can only be speculated, but S-wave velocity has been

determined to increase in materials with low saturation ratios, which are partly determined by soil moisture content, and decrease in materials with high saturation ratios (Irfan & Uchimura, 2013 and West & Menke, 2000). If the soil moisture content, which was observed to vary temporally within an earth embankment in Jackson et al. (2002), of the embankment is affected by the reservoir water level, then variation in the minimum spectral value of an HVSR trough might reflect changes in soil moisture content. This hypothesis would be best evaluated in another study employing the HVSR method in conjunction with a method to estimate soil moisture content such as Electrical Resistivity Tomography (ERT) at an earth embankment during varying water levels of the adjacent water body.

### **Conclusions**

The subsurface seismic structures of the Chestnut Hill Reservoir embankment in Massachusetts and Franklin Falls Dam in New Hampshire were estimated using the geophysical methods of HVSR, seismic refraction analysis, and MASW in addition to HVSR modeling. Paired with the surface layer shear-wave velocity estimates obtained from the MASW and seismic refraction analysis performed at the Chestnut Hill Reservoir, the fundamental frequencies obtained from the HVSR method proved effective at estimating the depth to bedrock from different measurement sites atop the reservoir embankment. The bedrock depths estimated by HVSR were within roughly 1 m of those obtained from MASW, which estimated the seismic structure of the embankment with better resolution than the seismic refraction analysis. There is more uncertainty in the estimated seismic structure of the Franklin Falls Dam relative to the Chestnut Hill Reservoir embankment because no other methods were employed at Franklin Falls to estimate seismic velocities of dam layers. Estimating depth to bedrock using a site's fundamental frequency requires the assumption of the average shear-wave velocity of the

materials above the reflecting bedrock surface, and so there is greater uncertainty in the estimation when a site's seismic velocities have not been validated by other methods such as MASW or seismic refraction analysis. Thus, the HVSR method is most effective for estimating the subsurface seismic structure of an earth embankment when used in conjunction with other geophysical methods to validate seismic structure properties.

The site fundamental frequencies observed in the repeated HVSRs calculated at the Chestnut Hill Reservoir embankment on different days from July 2021 to December 2022 varied by approximately 0.1 Hz to 0.7 Hz. Every HVSR at each embankment station contained a trough with an amplitude below 1.0 in the frequency band centered around  $2f_0$ . When running forward HVSR calculations in HV-Inv for both the Chestnut Hill Reservoir embankment and Franklin Falls Dam, the produced HVSRs only contain troughs when a low-velocity zone is included in the input seismic structure. This supports the notion that the presence of a sufficiently-wide trough with spectral values below 1.0 in an HVSR indicates a low-velocity zone below an observation site.

The observed fundamental frequencies did not vary significantly with varying water level, but the minimum spectral values of the troughs within HVSRs from noise measurements made at relatively low reservoir water levels had consistently higher values by more than one standard deviation compared to the average HVSRs from seismic noise measurements made at typical reservoir water levels about 6 ft higher. Increases in the minimum spectral value of the trough within the best-fit HVSR model for the Chestnut Hill Reservoir embankment were found by increasing the S-wave velocity of the low-velocity layer in the lower part of the embankment and decreasing the S-wave velocity of the thin, high-velocity layer in the upper part of the embankment relative to those velocities in the seismic structure estimated for the normal water

level. Varying reservoir water level might therefore affect seismic velocities within the embankment at a resolution measurable by the HVSR method.

This study has found the geophysical methods of HVSR, MASW, seismic refraction analysis, and HVSR modeling to be effective tools for estimating the subsurface seismic structure velocities, thicknesses, and densities of earth embankments. When used in conjunction with each other, the resolutions of the methods render them capable of detecting changes in the subsurface seismic structures of an earth embankment dam. Detecting changes in seismic structures of earth embankments is desirable because observing changes in seismic properties such as velocity could indicate zones of weakness within an embankment that could lead to failure. The methods employed in this study are also noninvasive, inexpensive, and quick to implement, making them not only effective but highly-desirable and practical options for monitoring the seismic structures of earth embankments.

## References

- Anomohanran, O. (2013). Seismic refraction method: A technique for determining the thickness of stratified substratum. *American Journal of Applied Sciences*, 10(8), 857.
- Bignardi, S. (2017). The uncertainty of estimating the thickness of soft sediments with the HVSR method: A computational point of view on weak lateral variations. *Journal of Applied Geophysics*, 145, 28-38.
- Billen, Magali. (2020, August 12). Seismic refraction (single layer). *LibreTexts Geosciences*, 5.2.1-5.2.5.
- Boston Landmarks Commission. (1989, September 26). *Chestnut Hill Reservoir and Pump Stations*. Retrieved February 24, 2023, from [https://www.cityofboston.gov/images\\_documents/Chestnut%20Hill%20Reservoir%20Pump%20Stations%20Study\\_tcm3-19719.pdf](https://www.cityofboston.gov/images_documents/Chestnut%20Hill%20Reservoir%20Pump%20Stations%20Study_tcm3-19719.pdf).
- Butterworth, S. (1930). On the theory of filter amplifiers *Wirel. Engineer*, 7(6), 536-541.
- Castellaro S. & Mulargia F. (2009). The effect of velocity inversions on H/V. *Pure and Applied Geophysics*, 166(4), 567–592. <https://doi.org/10.1007/s00024-009-0474-5>
- Cormier, V.F. Seismic attenuation: Observation and measurement. In *Geophysics Encyclopedia of Earth Science*; Springer: Boston, MA, USA, 1989.
- Dobrin, M.B. (1976). *Introduction to geophysical prospecting*. McGraw-Hill, New York, NY, 3rd ed.
- García-Jerez, A., Piña-Flores, J., Sánchez-Sesma, F. J., Luzón, F., & Perton, M. (2016, December). A computer code for forward calculation and inversion of the H/V spectral ratio under the diffuse field assumption. *Computers & geosciences*, 97, 67-78.

- Gorstein, M. & Ezersky, M. (2015). Combination of HVSR and MASW methods to obtain shear wave velocity model of subsurface in Israel. *International Journal of Georesources and Environment-IJGE*, 1(1), 20-41.
- Hildreth, J. L. (1899, April 14). *Distribution department, Chestnut Hill Reservoir, Effluent Gatehouse, Brighton, Mass., Apr. 14, 1899* [Photograph]. Digital Commonwealth. <https://ark.digitalcommonwealth.org/ark:/50959/qb98n177j>.
- Irfan, M., & Uchimura, T. (2013). Effects of soil moisture on shear and dilatational wave velocities measured in laboratory triaxial tests. In *Proceedings of the 5th International Young Geotechnical Engineers' Conference* (pp. 505-509). IOS Press.
- Kesarwani, A., Sharma, A., & Jain, C. (2012). MASW versus refraction seismic method in terms of acquisition and processing of data and the accuracy of estimation of velocity profiles. In *9th Biennial International Conference & Exposition on Petroleum Geophysics, Hyderabad* (Vol. 5).
- Lane, J. W., White, E. A., Steele, G. V., & Cannia, J. C. (2008, January). Estimation of bedrock depth using the horizontal-to-vertical (H/V) ambient-noise seismic method. *United States Geological Survey*. Retrieved February 28, 2023, from [https://water.usgs.gov/ogw/bgas/publications/SAGEEP2008-Lane\\_HV/](https://water.usgs.gov/ogw/bgas/publications/SAGEEP2008-Lane_HV/).
- Lee, M. W. (2003). *Velocity ratio and its application to predicting velocities*. Reston, VA, USA: *United States Geological Survey*.
- Liu, S. (2017). *Shear Wave Velocity Analysis by Surface Wave Methods in the Boston Area* (Doctoral dissertation, Boston College).
- Massachusetts Department of Conservation and Recreation. (2006, November 30). *Chestnut Hill Reservation Resource Management Plan*. Retrieved February 24, 2023, from

<https://www.mass.gov/service-details/chestnut-hill-reservation-resource-management-plan>.

- Moon, S. W., Subramaniam, P., Zhang, Y., Vinoth, G., & Ku, T. (2019). Bedrock depth evaluation using microtremor measurement: empirical guidelines at weathered granite formation in Singapore. *Journal of Applied Geophysics*, *171*, 103866.
- Nakamura, Y. (1989). A method for dynamic characteristics estimation of subsurface using microtremor on the ground surface. *Railway Technical Research Institute, Quarterly Reports*, *30*(1).
- Park, C. B., Miller, R. D., & Xia, J. (1998). Imaging dispersion curves of surface waves on multi-channel record. In *SEG technical program expanded abstracts 1998* (pp. 1377-1380). Society of Exploration Geophysicists.
- Pontrelli, M. (2020). Near surface shear wave velocity profile development in the Pioneer Valley and Tufts campus using a coupled HVSR-MASW technique.
- Sain, K., & Reddy, P. R. (1995). Direct calculation of thicknesses for high-velocity and underlying low-velocity layers using post-critical reflection times in a seismic refraction experiment. *Journal of applied geophysics*, *34*(2), 125-136.
- Simms, J. E., Doll W. E., Aguila E. T., Maniscalco S. J., & Wang, Y. (2022, April 2-6). Application of HVSR to levee composition and thickness assessments [Conference Presentation]. SAGEEP 2023/2nd Munitions Response Meeting, New Orleans, LA, United States.
- Tsai, C. C., & Lui, H. W. (2017). Amplification behavior of vertical motion observed from downhole arrays. In *Proceedings of the 16th world conference on earthquake*.

Xu, R., & Wang, L. (2021). The horizontal-to-vertical spectral ratio and its applications.

*EURASIP Journal on Advances in Signal Processing*, 2021, 1-10.

U.S. Army Corps of Engineers. (2021, May 4). *Franklin Falls Dam flood risk management project*. Retrieved February 24, 2023, from

<https://www.nae.usace.army.mil/Missions/Civil-Works/Flood-Risk-Management/New-Hampshire/Franklin-Falls/>.

U.S. Army Corps of Engineers. (2004, July 30). *General design and construction considerations for earth and rock-fill dams*. Retrieved April 19, 2023, from

<https://www.publications.usace.army.mil/>.

West, M., & Menke, W. (2000, February). Fluid-induced changes in shear velocity from surface waves. In *13th EEGS Symposium on the Application of Geophysics to Engineering and Environmental Problems* (pp. cp-200). EAGE Publications BV.